**Title**
Understanding river floods in the Rio Grande-Bravo Basin from 1900 to 2010



**Author**
Gómez Quiroga, Grace

**Publication Date**
2022

Peer reviewed|Thesis/dissertation

Understanding river floods in the Rio Grande-Bravo Basin from 1900 to 2010

By

GRACE GÓMEZ QUIROGA
THESIS

Submitted in partial satisfaction of the requirements for the degree of

MASTER OF SCIENCE

in

HYDROLOGIC SCIENCES

in the

OFFICE OF GRADUATE STUDIES

of the

UNIVERSITY OF CALIFORNIA

DAVIS

Approved:

---

Samuel Sandoval-Solis

---

Carlos E. Puente

---

Jonathan D. Herman

Committee in Charge

2023

# Acknowledgements

Many living beings helped me write this thesis and complete my degree. First, I want to thank Sam Sandoval, for trusting me and my timing –slowly, but surely. I thank my advisors Carlos Puente and Jon Herman, who consistently supported me in their courses and in writing this thesis. I thank my friends of the Water Management Lab for their enthusiasm, support, and guidance: Lau Garza, Ramón Saiz, Gabriela Rendón, Hervé Guillon, Noelle Patterson and Jeneya Fertel. I thank my colleagues at the Spanish Department: Claudia Hernández, Paula Plastic and Angelica González; by working with you I learned that I love to teach. I thank my Spanish 1 students; I keep your vulnerability and appreciation in my heart. I thank my peers of the Hydrologic Sciences Graduate Group for their fellowship and encouragement: Nusrat Molla, Yara Pasner and Rachel Kennard. I thank my peers of the UC Davis chorus for the music we shared. I thank the Student Disability Center at UC Davis for providing me with accommodations, so I am fairly evaluated by my academic contributions. I thank my advisors at Fulbright-Garcia Robles and the Institute of International Education, who provided funding and guidance through the pandemic.

I thank my best friend, Sofi Narro, who always believed I would pull through this master's program. I thank my therapist for guiding me compassionately during the most difficult times and for helping me discover my Self. I thank my parents for their unwavering support, in the good times and the bad. I thank my friends in México: Jesús Salas, Cristi Nieto, Iván Hernández, Franco Quiroga, for the text messages, long phone

calls, and all TV shows and movies we watched remotely. I thank my aunt and uncle Isabel Goode and Winston DeBlanc, for hosting and supporting me. I thank my dog Mila, for keeping me company during the hardest of times, for making me laugh, and for not eating poop *that* often.

I thank Putah Creek in south Davis, for welcoming me and keeping me company during the first year and a half of the pandemic. I thank the giant sequoias at Yosemite National Park, for teaching me about resilience during crises. I thank the California coast for renewing my spirit with a fresh breeze. I thank my hometown for welcoming me back, with their beautiful beach, lagoons and river.

# Abstract

The Rio Grande-Bravo (RGB) Basin, shared by the United States and Mexico, is a water-scarce basin shaped by climatic, topographic, and ecosystemic contrasts. As part of the natural flow regime, floods support habitat creation by resetting the channel, regulating water quality, and controlling invasive species. However, since 1870 the region has faced considerable socioeconomic growth, which has heavily altered the natural hydrology, resulting in drastic degradation of river health.

This research analyzes natural and regulated flood events in the Southern branch of the RGB Basin from 1900 to 2010 at six control points. Flood timing was described with central metrics and measures of spread, which were also used to compare differences between natural and regulated floods. Flood magnitude and frequency were analyzed using flood frequency analysis and magnitude prediction of the 2-, 5-, and 10-year floods. To compare magnitude and frequency of natural and regulated floods, two indexes were developed.

The main findings are: (1) natural flood timing reflects the climatic drivers of two main headwaters: flood events during the snowmelt season in the northern branch above the cities Presidio and Ojinaga, and during the monsoon and tropical storm season in the southern branch; (2) in the regulated regime, floods occur earlier in the year, most notably at the basin outlet; (3) natural median floods range from 720 $m^3/s$ at the headwaters to 2,250 $m^3/s$ at the basin outlet; (4) regulated median flood magnitudes

decrease 70% in four stations, with larger floods occurring in stations located upstream the river outlet, opposite to natural hydrology; (5) the 10-year natural flood estimates range from 2,055 $m^3/s$ to 6,083 $m^3/s$; (6) natural flood estimates show a pattern of dry and wet periods; and (7) frequency of large floods decrease at all stations, most noticeably after 1960.

Changes in flood timing, magnitude, and frequency have significant implications for physical, biogeochemical, and biological ecosystem functions. The life stages of several species are timed with floods, like fish spawning and migration. Physical and biogeochemical functions triggered by predictable, large floods support habitat creation by regulating water quality, preventing channel narrowing, depositing nutrients in the floodplain, and clearing out invasive species, amongst many other functions. Water management alternatives to reproduce functional flows, especially floods, have already been proposed by several authors, showing it is possible to restore ecological functions and satisfy human water management goals.

# Contents

# 1 Introduction

Climate variability results from the interactions between the components of the Earth system, including the atmosphere, hydrosphere, and biosphere (Hernández et al., 2020). Droughts and floods, amongst heat waves and cold spells, are some of the hydroclimatic extremes that result from this naturally occurring dynamism (Dadson et al., 2019).

Droughts and floods shape the evolution and health of river and riparian ecosystems across all types of basins (Parasiewicz et al., 2019). The Natural Flow Regime (NFR), a paradigm for river restoration and conservation, proposes that "the ecological integrity of river ecosystems depends on their natural dynamic character" (Poff et al., 1997). Given that river and riparian species evolve with and adapt to this environmental variability, they can "persist in the face of seemingly harsh conditions, such as floods and droughts, that regularly destroy and re-create habitat elements" (Poff et al., 1997).

Floods occur when water rises to overflow land that is not usually submerged (Hewlett, 1982). More specifically, river floods arise when a flow is too large to be contained within the natural channel network (Hewlett, 1982). Even though these events are usually associated with risks to human lives and infrastructure, they have a wide array of ecological functions. For example, floods shape physical habitats in the channels and on the floodplain (e.g. lateral channels, oxbow lakes), provide migration and spawning cues for fish, and provide plant seedlings with prolonged access to soil moisture, amongst many other functions (Arthington, 2012).

Most rivers and floodplains, however, have been modified by humans. Water diversions, reservoir operation, river channelization, and land use change, amongst many other human interventions, have altered the natural flow regime, the channel, and the floodplain of many rivers throughout the world, as well as their connections to groundwater and wetlands (Arthington, 2012). This has resulted in unprecedented freshwater biodiversity loss and increasing damages and risks to human lives and infrastructure.

In semi-arid basins, in particular, floods play a crucial role for river and riparian ecosystem health (Arthington, 2012). These basins are characterized by a high level of climate variability; they experience consistent, year-long dry periods marked by punctuated precipitation events, which vary greatly from year to year. Long periods of low flows dehydrate channel habitats and isolate water bodies, which are filled and reconnected during infrequent and low predictable high flows and floods (Arthington, 2012).

Human and ecological systems in semi-arid basins face many challenges, including overall ecosystem degradation and hydrologic alteration. These basins support 1.1 billion people worldwide (Scholes, 2020), and they are prone to extensive water and land degradation. This degradation results from the "over-optimistic expansion of crops or herds during periods of rainfall abundance, followed by their collapse in times of multi-year drought" (Scholes, 2020).

The Rio Grande-Bravo Basin (RGB) is a semi-arid basin shared by Mexico and the United States. It is the fifth longest river in North America -approximately 3,000km-, it is home to 10.4 million people, and its drainage area is 557,000 km2, covering three states in the United States (Colorado, New Mexico, and Texas) and five states in Mexico (Durango, Chihuahua, Coahuila, Nuevo León, and Tamaulipas) (Sandoval-Solis et al., 2022).

Since the late 1800s, the region has faced drastic environmental and socioeconomic changes, which have had lasting effects in river and riparian biodiversity. Economic activities, especially agricultural development, have resulted in severe impacts to river ecosystems, like channel narrowing and water pollution, and hydraulic infrastructure has considerably altered the natural flow regime of the basin (Blythe & Schmidt, 2018). Several fish species are extinct, like the Rio Grande shiner, phantom shiner, and the Rio Grande bluntnose shiner, while others are endangered, like the Rio Grande chub and Rio Grande silvery minnow) (Bilbe, 2006).

## 1.1 Research gap, objectives and hypothesis

Until recently, there were no daily streamflow records of the natural hydrology in the RGB; the existing data only captured the regulated streamflow. However, in 2018 Blythe and Schmidt (Blythe & Schmidt, 2018) computed the natural daily streamflow of the Northern branch of the RGB, including the river mainstem and tributaries. The Northern branch encompasses the river mainstem from its headwaters in Colorado until it reaches the outlet of its main tributary, Rio Conchos. Likewise, Garza-Díaz and Sandoval-Solis (Sandoval-Solis et al., 2022) obtained the natural daily streamflow in the

Southern branch of the RGB. The Southern branch RGB includes the river mainstem and its confluence with Rio Conchos and the outlet of the river in the Gulf of Mexico. These natural streamflow records span from the late 1880s until 2015.

This new data presented an opportunity to describe naturally occurring floods in the Southern branch of the RGB during the last 110 years. This characterization would provide a clearer picture of recent natural flood events characteristics and how they have changed in the regulated basin. Additionally, it would be possible to understand the relationship between floods and climate variability in the last century, considering the natural streamflow as a proxy for climate.

Hence, the overall goal of this thesis is to characterize flood events in the RGB from 1900 to 2010. The hypothesis that supports this work is that it is possible to estimate flood characteristics, particularly timing, magnitude, and frequency, using daily natural and regulated streamflow data; that it is feasible to make a quantitative comparison between the natural and the regulated flood events; and that it is possible to understand how floods have changed depending on the prevalent climate conditions in the basin.

The specific objectives of this project are:

1. To describe 1-day annual peak flows for natural and regulated hydrology in terms of magnitude, frequency, and timing (quantitative).
2. To compare the natural and regulated peak flow characteristics (quantitative).

3. To elaborate on how the change on peak flows affects the environment (qualitative).

This research study applies traditional flood characterization techniques for the first time to the Southern branch of the Rio Grande for a long period of record (1900-2010), for both natural and regulated streamflow conditions. This analysis describes flood events in terms of timing, magnitude and duration, and allows comparison between natural and regulated streamflow conditions.

# 2 Literature review

## 2.1 Ecological functions of floods

As mentioned in the introduction, the Natural Flow Regime (NFR) is a paradigm for river restoration and conservation. This paradigm poses that streamflow is a "master variable" of river health; streamflow is "strongly correlated with many critical physicochemical characteristics of rivers, such as water temperature, channel geomorphology and habitat diversity…, [which] limit the distribution and abundance of riverine species and regulates the ecological integrity of flowing waters." (Poff et al., 1997).

The NFR establishes five components of the flow regime that regulate ecological processes: magnitude, frequency, duration, timing, and rate of change (Poff et al., 1997). Magnitude refers to the amount of water flowing in the river channel per unit time; frequency refers to how often a flow above a certain magnitude recurs over some period of time; duration is the period of time associated with a specific flow condition; timing refers to the regularity with which a flow of defined magnitude occurs; while rate of change refers to how quickly flow changes from one magnitude to another (Poff et al., 1997). These five components can be used to describe the "entire range of flows that sustain the integrity of river and riparian ecosystems" (Poff et al., 1997). High flows and floods can be described in terms of these components. Table 1 provides several examples of the ecological functions of high flows and large floods.

Another paradigm relevant to streamflow and ecosystem health is the Flood Pulse Concept (FPC). This paradigm refers to the vital role of the annual flood cycle:

> "The ecology of unmodified floodplain rivers is governed almost entirely by the pulsing of the predictable annual flood cycle. These pulses maintain the system in a state of dynamic equilibrium in which organisms and processes respond to the rate of rise and fall and the amplitude, duration, frequency, and regularity of the flood pulses. During flooding, high habitat diversity on the inundated floodplain is coupled with massive increases in the area of aquatic habitat, nutrient regeneration, and increased primary and secondary productivity" (Arthington, 2012).

Floods play a crucial role in the health of river and riparian ecosystems. Due to floods "nutrients are replenished, fish reproduction and dispersal become possible on a grand scale, and fisheries productivity of inundated floodplains reaches “boom” proportions" (Balcombe et al., 2007; Bunn et al., 2006). Additionally, these processes "maximize the chances of floodplain and channel water bodies starting the dry season with a diverse, abundant, and healthy fish assemblage immediately after flood recession, and this ultimately enhances the survival of fish and other biota through prolonged periods of adverse conditions” (Arthington & Balcombe, 2011; Walker et al., 1995).

Table 1. Ecological functions of high flows and large floods (Arthington, 2012).

| Flow magnitude | Ecological functions |
|---|---|
| **High flows** | Shape physical character of river channel, including pools, riffles, runs<br>Determine size of streambed substrates (sand, gravel, cobble)<br>Prevent riparian vegetation from encroaching into channel<br>Restore normal water-quality conditions after prolonged low flows, flushing away waste products and pollutants<br>Aerate eggs in spawning gravels, prevent siltation<br>Provide suitable habitats for invertebrates and fish<br>Maintain suitable salinity conditions in estuaries |
| **Large floods** | Shape physical habitats in channels and on floodplain (e.g., lateral channels, oxbow lakes)<br>Provide migration and spawning cues for fish, trigger invertebrate life-history phases<br>Enable fish to spawn on floodplain, provide nursery habitat for juvenile fish<br>Provide new feeding opportunities for fish, amphibians, waterbirds<br>Distribute life stages of fish and invertebrates among channel habitats<br>Create sites for recruitment of colonizing plants<br>Provide plant seedlings with prolonged access to soil moisture<br>Maintain diversity in floodplain plant and forest types through differential inundation<br>Disburse seeds and fruits of riparian plants<br>Flush organic materials (food) and woody debris (habitat structures) into channel<br>Purge invasive, introduced species from aquatic and riparian communities<br>Maintain suitable salinity conditions in estuaries<br>Provide nutrients and organic matter to estuaries<br>Stimulate spawning of estuarine biota and support recruitment |

## 2.2 Flood events characteristics

### 2.2.1 Flood magnitude and frequency

There are several techniques for analyzing and predicting floods, which can be grouped in four categories: flood frequency analysis, flood duration prediction, flood routing, and catchment modeling (Watson & Burnett, 2017). Flood frequency prediction consists of statistical and graphical methods to determine the probability of recurrence of peak flows using long-term streamflow records. Flow duration prediction is an extension of the previous technique, showing what percentage of time a streamflow is likely to be greater than a desired value. Flood routing includes several methods that predict flood level in downstream locations based on observed flood discharge or precipitation events occurring upstream. Lastly, catchment modeling uses hydrologic variables - precipitation, evaporation, infiltration rate, groundwater and surface interactions, amongst others- to predict flooding event characteristics.

Flood frequency analysis uses empirical or analytic probability distributions to describe possible magnitudes and frequencies of peak flows (Teegavarapu et al., 2019). Using analytic distributions has several advantages (Stedinger & Foufoula-Georgiou, 1993): they provide a smooth interpretation of the empirical distribution with more accurate statistics; they present a compact and accessible representation of data; they provide a more realistic probability of occurrence; and they allow to estimate the probability of events that lie outside of the data sample in terms of either magnitude or frequency.

The main limitations of flood frequency analysis are: (1) that "the fitting of any model requires an *a priori* assumption about the underlying distribution generating flood events" (Kidson & Richards, 2005) and (2) the streamflow record -which rarely exceeds 100 years and is often shorter than 30 years- will not capture all flood events, especially extreme ones (Teegavarapu et al., 2019). Nevertheless, there are several methods for extending records, including the techniques mentioned above, as well as supplementing the recorded data with historical and paleoflood information (Kidson & Richards, 2005).

Fitting an analytic model for flood frequency analysis consists in three steps: choosing the data, choosing the model, and estimating parameters (Bobée et al., 1993). Table 2 presents alternatives for these three steps. The choice of model is usually a debated subject; since flood frequency analysis informs planning and insurance, which involve legal liabilities, there are standards in several countries, including the United States, where log-Pearson Type III (LP3) is the official model, and the United Kingdom, where the generalized Logistic is used (Kidson & Richards, 2005). However, none of these models have a hydrological theoretical basis and standardization assumes a one-size-fits-all approach.

For estimating flood risk where liabilities are involved, two recommendations are (1) to compare flood frequency analysis obtained with different models to assess the best fit (Haktanir & Horlacher, 1993), performing goodness-of-fit tests appropriate for each model, and (2) using the Power Law model; recent evidence suggests this distribution is suitable to describe extreme natural events, such as earthquakes, volcanic eruptions,

landslides, avalanches, and forest fires (Kidson & Richards, 2005). Given the standardized use of LP3 in the United States, this model is described below.

Table 2. Examples of choices of data, models, and parameters for flood frequency analysis. Adapted from Kidson and Richards (2005).

| Step | Examples |
|---|---|
| **Data choice** | Series of annual maximum discharge recorded at a gaging station.<br>Partial series of peak discharge over a set threshold.<br>Additional, discrete data from historic and paleoflood records. |
| **Model choice** | 2-parameter models (location and shape): log normal (LN2), Gumbel Extreme Value type 1 (EV1). Advantages: simplicity and ease of fit.<br>3-parameter models (location, shape and scale): log Pearson type III (LP3), generalized extreme value (GEV). Advantages: flexibility to fit more catchment records and larger scales.<br>Other models: gamma distribution family, Weibull, extreme value family, logistic distribution family, power law. |
| **Parameters estimation** | Method of moments: mean, variance, skew.<br>L-moment method: defines characteristics of a sample based on combinations of the difference between two randomly selected events.<br>Maximum likelihood: parameters are optimized via a search through parameter space, can be applied to multimodal probability density functions. |

The LP3 distribution is widely used in the United States, being the standard for flood frequency analysis used by federal agencies. The technique is outlined in Bulletin 17C, published in May 2019 (England et al., 2018). In the previous guidelines, Bulletin 17B (Interagency Advisory Committee on Water Data, 1982), the recommendation was to fit a Pearson Type III distribution to the logarithm of the values of the annual flood series,

using the method of moments to estimate population parameters -mean, variance, and skew.

The major features of the updated guidelines, Bulletin 17C, are estimation of regional skew coefficients, adjustment of low outliers, historical flood peaks, an extension of the method of moments to include interval data, amongst others. A main concern when using the LP3 function is the upper limit distinctive of this distribution, which bounds the value of outlier, extreme flood events. In spite of this limitation, it has been found that "the characteristics of real US flood data across the 14 regions delineated by the US Geological Survey fall well within the range of parameters for which the LP3 distribution is thought to produce reasonable flood-like distributions" (Teegavarapu et al., 2019).

Mean, standard deviation, and skew coefficient ($X$, $S_x$, $G_x$) are computed as follows:

$$\bar{X} = \frac{1}{N}\sum_{i=1}^{N} X_i\,; \quad S_x = \left[\frac{1}{N-1}\sum_{i=1}^{N}(X_i - \bar{X})^2\right]^{1/2}; \quad G_x = \frac{N}{(N-1)(N-2)S^3}\sum_{i=1}^{N}(X_i - \bar{X})^3$$

The parameters of the Pearson Type III distribution ($\alpha$, $\beta$, $\tau$) are obtained by:

$$\hat{\alpha} = \frac{4}{G_x^2}; \qquad \hat{\beta} = \frac{S_x G_x}{2}; \qquad \hat{\tau} = \bar{X} - \hat{\alpha}\hat{\beta} = \bar{X} - 2\frac{S_x}{G_x}$$

Several methods exist to assess the goodness of fit of the analytical distribution to the observed data, including the probability plot correlation coefficient (PPCC), and the Kolmogorov-Smirnov test. The probability plot correlation coefficient (PPCC) is a test for normality. It assesses the linear correlation coefficient between data and their normal quantiles (Helsel et al., 2020). Samples from a normal distribution will have a correlation

coefficient very close to 1.0. As data depart from normality, their correlation coefficient will decrease below 1. The probability plot is the graphical analog of the PPCC, which visually represents the results of the PPCC. It presents how the data departs from normality (Helsel et al., 2020). The Kolmogorov-Smirnov test is a nonparametric test for the appropriateness of a distribution (Mimikou et al., 2016). It computes the difference between a cumulative distribution function and the observed cumulative histogram, or, in other words, it quantifies the distance between the empirical distribution function of observed data and the cumulative distribution function of a reference distribution.

Another method to analyze flood frequency and magnitude is the exceedance probability curve. The variable in question is plotted in one axis, arranged from lowest to largest value, ranked by a selected plotting position, while cumulative frequency is plotted in the other axis, with values from 0 to 1. To rank the values, several authors have proposed different plotting positions, such as Weibull (1939), Blom (1958), and Cunnane (1978). These plots present several advantages to other methods: (1) arbitrary categories are not required, (2) all of the data are displayed, and (3) every point has a distinct position without overlap (Helsel et al., 2020).

### 2.2.2 Flood timing

Before the late 1970s, flood analysis and prediction were often limited to understanding flood magnitude and frequency. These studies were usually intended for land-use planning and infrastructure: to identify sustainable land development options; to design water use and water control projects; to establish floodplain definition and

management; and to design transportation infrastructure (Teegavarapu et al., 2019). However, as river restoration and protection were prioritized by scientists and natural resource managers, environmental flows science and management emerged and introduced timing as a relevant variable to understand the natural flow regime.

As aforementioned, in the NFR paradigm timing is a relevant component for river health, which is defined as the regularity with which a flow of a certain magnitude occurs (Poff et al., 1997). More recently, the functional flows approach was proposed for heavily modified rivers to "retain specific process-based components of the hydrograph" instead of replicating the full natural flow regime of a river (Yarnell et al., 2015). Some functional flow components include wet-season initiation flows, peak magnitude flows, spring recession flows, dry-season low flows, and interannual variability.

The timing of wet-season initiation flows and of peak magnitude flows is crucial. Wet-season initiation flows mark the transition between dry season and wet season conditions. These flows "typically have higher suspended sediment concentrations", which provide "key life-history cues" like migration and spawning to native species (Yarnell et al., 2015). Likewise, peak magnitude flows provide spawning and migration cues, "as well as the flow volume needed to create a migration corridor" (Yarnell et al., 2015).

> "The timing of a peak magnitude flow should occur within the natural season of high flows when native species have life-history strategies to survive and even

> capitalize on these large-scale floods. [...] Shifts in the timing of peak flows, particularly to seasons that naturally might be dominated by low flows, can be detrimental to the life-history strategy of these native species." (Yarnell et al., 2015).

Likewise, according to the functional flows approach, the magnitude and frequency of wet-season initiation flows and peak magnitude flows fulfill the following functions:

> "The magnitude of an initiation flow should be such that connectivity with the riparian zone is established and organic matter can be flushed from the channel substrate. On many rivers, such flushing flows that remove sand from riffles and organic fines from pools and riparian edgewaters can be effective at or above 60% bankfull depth."

> "The magnitude of a peak flow should be large enough to mobilize bed material and maintain in-channel bar forms, connect to overbank areas and floodplains, and occur with a frequency of 1–3 years depending on regional climate conditions. Very large magnitude peak flows that cause extensive floodplain scour and fill and reset floodplain vegetation succession naturally occur every 10–20 years."

# 3 Methods

The methods are grouped in two steps: flood event description and comparison of natural and regulated flood events. First, the natural and regulated annual flood series were obtained to estimate flood timing, magnitude, and frequency through different statistical analyses. Then, these three characteristics of natural and regulated flood events are estimated. Lastly, the flood characteristics are compared with population metrics and indexes.

## 3.1 Data

For the Northern branch of the RGB, the daily natural streamflow data estimated by Blythe and Schmidt (Blythe & Schmidt, 2018) was used. Their model employed a mass-balance equation and observed data including regulated daily streamflow, reservoir storage, and water imports data. Embudo, Otowi Bridge, San Marcial, and Presidio are four of the seven primary long-term stations they used in the mass-balance model. These stations are located in the river mainstem, and they capture a significant trend in peak flow timing, magnitude, and frequency. Since this thesis addresses floods in the Southern branch of the RGB, the results only include Presidio station, as well as the stations located in the Southern branch. However, figures for Embudo, Otowi Bridge, and San Marcial are presented in supplemental materials.

For the Southern branch, the daily natural streamflow data estimated by Garza-Díaz and Sandoval-Solis (2022) was used. Similarly, streamflow was obtained with a mass-balance

model using observed data including regulated daily streamflow, reservoir storage, water imports, precipitation, and temperature. The stations included in the Southern branch are: Rio Conchos, Below Ojinaga, Foster Ranch, Amistad, Laredo, and Anzaldúas. All stations are located in the river mainstem except for Rio Conchos, which is located at the outlet of Rio Conchos, the tributary.

For the regulated streamflow in the Northern and Southern branch of the RGB, data was obtained from three sources. For Embudo, Otowi Bridge, and San Marcial, the data used were observed (regulated) streamflow data obtained by the United States Geological Survey (USGS). For the Southern branch, including Presidio, the data used was obtained by the International Boundary and Water Commission (IBWC) and the Mexican National Water Agency (Comisión Nacional del Agua, CNA). Table 3 presents the names of gaging stations, station number, and agency that collects streamflow data, Figure 1 presents the availability for both natural and regulated streamflow data, and Figure 2 shows the location of all gaging stations.

Table 3. Streamflow gages of the control points considered in this research.

| Station | Station name | Agency | Station number |
|---|---|---|---|
| **Embudo** | Rio Grande at Embudo, NM | USGS | 08279500 |
| **Otowi Bridge** | Rio Grande at Otowi Bridge, NM | USGS | 08313000 |
| **San Marcial** | Rio Grande at San Marcial, NM | USGS | 08358500 |
| **Presidio** | Rio Grande above Rio Conchos near Presidio, TX and Ojinaga, Chih. | IBWC | 08-3715.00 |
| **Río Conchos** | Rio Conchos, Chih. | CNA | 24388 |

| Station | Station name | Agency | Station number |
|---|---|---|---|
| **Below Ojinaga** | Rio Grande below Rio Conchos near Presidio, TX and Ojinaga, Chih. | IBWC | 08-3742.00 |
| **Foster Ranch** | Rio Grande at Foster Ranch near Langtry, Texas and Rancho Santa Rosa, Coah. | IBWC | 08-3772.00 |
| **Amistad** | Rio Grande below Amistad Dam ear Cd. Acuna, Coah. and del Rio, TX | IBWC | 08-4509.00 |
| **Laredo** | Rio Grande at Laredo, TX and Nuevo Laredo, Tamps. | IBWC | 08-4590.00 |
| **Anzaldúas** | Rio Grande below Anzaldúas Dam near Reynosa, Tamps. and Mission, TX | IBWC | 08-4692.00 |

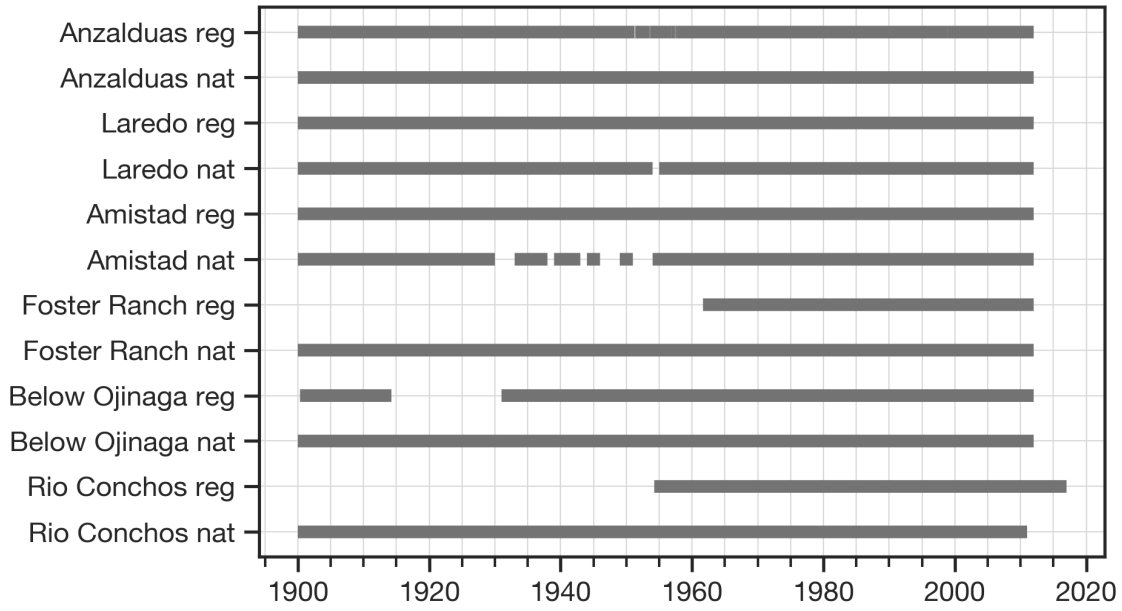


Figure 1. Daily streamflow data availability for relevant streamflow gauges (1900 – 2017).


Figure 2. Location of streamflow gages.

## 3.2 Flood events characteristics

### 3.2.1 Timing

Flood or peak flow timing refers to the day of the calendar year in which the annual maximum streamflow occurs. The annual peak flow and its ordinal date of occurrence (i.e., day of the year, ranging between 1 and 366) were computed from the daily natural and daily regulated streamflow series. Next, descriptive statistics were computed, including central metrics (average and median), measures of spread (standard deviation, interquartile range), and maxima and minima. Then, peak flow timing was

plotted in violin plots in different time windows: the complete 110-year data set and periods of 25 years.

### 3.2.2 Magnitude and frequency

Flood or peak flow magnitude is simply the value of the maximum streamflow that occurs in one day in a given calendar year, expressed in cubic meters per second. Frequency refers to the probability with which a peak flow of a certain magnitude occurs. Two methods were used to estimate natural and regulated flood magnitude and frequency: flood frequency analysis and flood magnitude prediction.

#### *Flood frequency analysis - Exceedance probability curves*

First, exceedance probability curves were drawn by plotting cumulative frequency against streamflow magnitude. To construct these plots, the one-day annual peak flow data were ranked from smallest (i = 1) to largest (i = n, where n = sample size). Next, plotting positions that better centers long time series data were computed as a function of rank i and sample size n, where $\frac{(i - 0.4)}{(n + 0.2)}$ (Cunnane, 1978). This technique for obtaining plotting positions was chosen since it better centers long term data records. Thus, exceedance probability curves were drawn for the complete 110-year data set, with peak flow magnitude in the horizontal axis and cumulative frequency in the vertical axis. Additionally, the curves were drawn in a double logarithm plot, both the x-axis and the y-axis, to observe if the empirical distribution follows the Power Law.

### *Flood magnitude prediction - Log-Pearson Type III*

Flood magnitude estimates were predicted by fitting a Pearson Type III distribution to the logarithm of the annual peak flow dataset, using the mean, standard deviation and skew coefficient of the data, and the method of moments. This fitting was performed for (1) the complete 110-year time series to obtain the cumulative distribution function, and (2) in consecutive windows of 20 years (i.e., 1900 - 1920, 1901 - 1921, …, 1994 - 2014) to obtain the 2-, 5-, 10-year annual peak flow estimates.

To assess the goodness of fit of the distribution to the sample data, two techniques were used: probability versus quantile plots with 5% and 95% confidence intervals and the probability plot correlation coefficient (PPCC) with its graphical analog, the quantile-quantile plot. The quantile-quantile plot graphs observed quantiles in the y-axis versus theoretical quantiles in the y-axis.

## 3.3 Comparison of natural and regulated peak flows

### 3.3.1 Change in timing

To compare the differences in flood timing between natural and regulated flows, three techniques were used: the Wilcoxon signed-rank test, estimating differences in the central metrics (average, median), and computing differences in measures of spread (standard deviation and IQR).

### 3.3.2 Change in magnitude

To assess the change in magnitude, the 10-year estimate of regulated peak flow of a determined year was divided by the 10-year estimate of the natural peak flow of the same year. The 10-year estimates were obtained with the log-Pearson Type III function in windows of 20-years. The question this index seeks to answer is: what is the fraction of the regulated flood magnitude compared to the natural flood magnitude? For example, an Index 1 of 0.5 means that the regulated flood magnitude is 50% of the natural flood magnitude.

$$Index\ 1 = \frac{Flood\ magnitude_{regulated}^{T=10}}{Flood\ magnitude_{natural}^{T=10}}$$

### 3.3.3 Change in frequency

To assess the change in frequency, two steps were involved. First, the magnitude of the natural flood with a 10-year return period was obtained for each year using the LP3 function in windows of 20 years. Then, the estimates of the regulated flood magnitude were computed with the LP3 function and the 110 year regulated flood data. The value of the natural flood magnitude was looked up in the 110 year regulated estimates, and the frequency of the regulated estimate was obtained. For example, for a given station, from 1900 to 1920, the natural peak flow estimate with a 10-year return period is 300 $m^3/s$. This value, 300 $m^3/s$, was looked up in the quantiles obtained with the LP3 function of the 110-year regulated peak flow data. The frequency of the 300 $m^3/s$ in the regulated flood estimates is a return period of 50 years. The questions this index seeks to answer are: how often do natural flood magnitudes occur in the regulated hydrology and how

does this frequency compare to the frequency of natural floods? For example, an Index 2 of 5 (=50/10, using the example from above) means that a flow of 300 $m^3/s$ in the regulated streamflow used to occur five times more often in the natural regime.

$$Index\ 2\ = \frac{P(Q_{nat\ (T\ =\ 10)})\ \in\ TS_{natural,t\ =\ 20\ years}}{P(Q_{nat\ (T=10)})\ \in\ TS_{regulated,t\ =\ 110\ years}} = \frac{F_{natural}}{F_{regulated}}$$

Frequency is obtained as follows, where F is frequency, P is percentile, and T is return period. Figure 3 presents a conceptual model that illustrates how to obtain the frequencies to compute Index 2.

$$F\ = \frac{P}{100} = 1\ -\ \frac{1}{T}$$

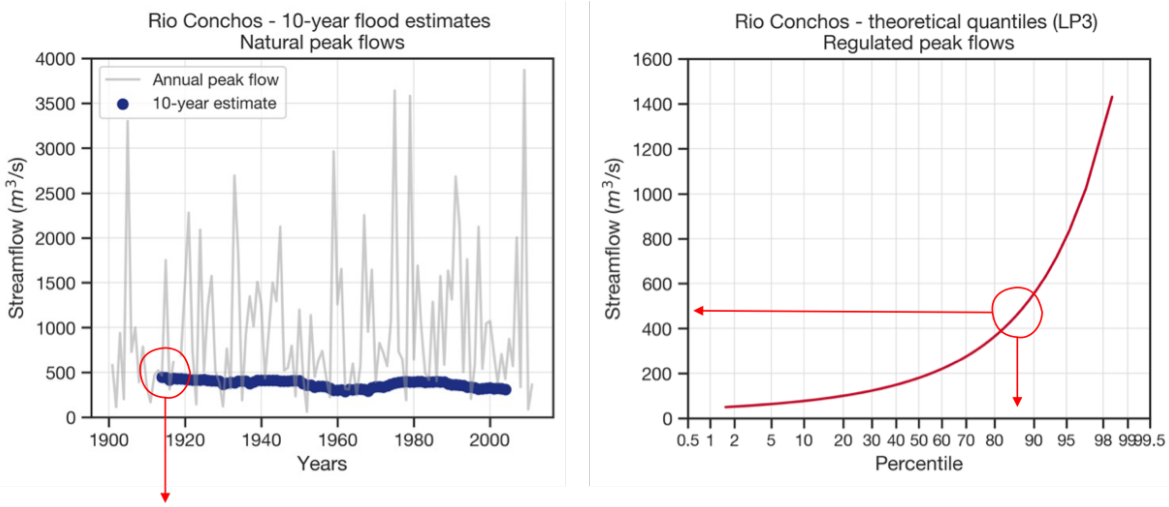


Figure 3. Conceptual calculation of Index 2.

# 4 Case study: Rio Grande-Bravo Basin

The climate and topography in the RGB shape a land of contrasts, from high elevations in the subarctic mountains, to hot, semi-arid deserts and river canyons, to semiarid coastal plains. The headwaters of the RGB are located in the San Juan Mountains, Colorado, where the climate is subarctic, with cool summers and year-round precipitation, feeding streamflow through snowmelt (Beck et al., 2018). The river continues downstream through the cold semi-arid dryland, with very few additional discharges from small tributaries (Blythe & Schmidt, 2018). Then, at the Mexico and United States border, the river receives water from the main Mexican tributary, Rio Conchos, which flows from the semi-arid, cold Sierra Madre Oriental in Chihuahua. Streamflow in this area is generated by several processes, including the North American monsoon and tropical storms (Sayto Corona et al., 2017; Woodhouse et al., 2012). The river continues through hot deserts and semi-arid plains until it reaches coastal plains and the Gulf of Mexico, with some additional inputs from tributaries, including the Pecos River, with its headwaters in New Mexico.

The RGB basin shares key climatic features of semi-arid basins. These are (1) high mean daytime temperatures, (2) low atmospheric humidity and rainfall, which occurs mostly as discrete convective storms, (3) intraannual rainfall seasonality, marked by wet summers and dry winters, and (4) high interannual rainfall variability, due to modes of climate variability, like the El Niño Southern Oscillation (Scholes, 2020). Thus, the RGB basin experiences long periods of water scarcity and brief events of water abundance.

In fact, semi-arid basins are capable of enduring prolonged droughts and they experience pulse responses to precipitation events, such pulses are "rapid changes in the land-atmosphere exchanges of energy, water, and carbon" (Bastos et al., 2022).

### 4.1.1 Floods in the Rio Grande-Bravo Basin

Floods in the Southern branch play a vital role in sustaining riparian and river health. As part of the natural hydrology, they sustain the features and processes of the river channel and floodplain that support habitat creation, including resetting the channel, regulating water quality, controlling invasive species, and transporting nutrients to the floodplain (Garza-Díaz, 2022). Table 4 provides a list of ecological functions of high flows and floods. The ecological functions are categorized by functional flow components: dry season baseflows, summer pulse flows, monsoon peak flows, wet season high flows, and snowmelt flows, and for each ecological function the natural flow regime components involved are indicated.

Table 4. Ecological functions of the functional flow components of the Rio Grande-Bravo Basin (Garza-Díaz, 2022).

| Functional Flow Component | Ecosystem Function Type | Function/ Process | Associated Flow Characteristic | References |
|---|---|---|---|---|
| Dry-season baseflow | Physical | Sediment accumulation on the channel bed | M, D | Dean et al., 2011; Escobar-Arias and Pasternack, 2010 |
| | | Maintain water table levels and soil moisture | M, D | Postel and Richter 2003 |
| | Biogeochemical | Nutrient enrichment concentration | M, D | Ning et al., 2010 |
| | | Maintain water temperature and dissolved oxygen | M, D, T, R | Postel and Richter 2003 |
| | Biological | Support conditions for spawning | M, D, T | Heard 2012; WWF 2009 |
| | | Enhanced growth rates of planktonic algae, followed by rapid growth and turnover of zooplankton | M, D, T | Humphries et al., 2020 |
| | | Concentration of prey for native predators | M, D, T | Ning et al., 2010 |
| | | Maintain habitat patches for reproduction of native fishes | M, D, T | Falke et al., 2010; Gido and Propst 2012 |
| | | Fish establishment and defending of nests | M, D | WWF 2009 |
| Summer pulse flow | Physical | Sediment deposition and construction of levees | M, D, F | Dean et al., 2011; Filgueira-Rivera et al., 2007 |
| | | Bank scouring | M, D, F | Dean et al., 2011 |
| | Biogeochemical | Increase photosynthetic gas exchange | M, D | Fravolini et al., 2005 |
| | | Modify salinity conditions in estuaries | M, D | Postel and Richter 2003 |
| | Biological | Provides cues for fish migration | M, D, T | WWF 2009 |
| | | Support conditions for spawning | M, D, T | Heard 2012 |
| | | Aerate eggs in spawning sites | M, D | Postel and Richter 2003 |
| Monsoon peak flows | Physical | Channel reset, avulsions, and braiding | M, D, F | Ashworth et al., 2004; |
| | | Meander migration and cutoffs | M, D, F | Harrison et al., 2011; Swartz et al., 2020 |
| | Biogeochemical | Increase in soil microbial response and flux of carbon and nitrogen pools | M, T, F | Austin et al., 2004 |
| | | Deposit nutrients on floodplain | M, D | Postel and Richter 2003 |
| | Biological | Growing period for riparian plants | M, D, T, R | Williams et al., 2006 |
| | | Removal of generalists and survival of native species | M, D | Heard 2012 |
| | | Insect larvae coloniztion | M, D | Kimura 2011 |
| Wet season high flows | Physical | Mainteined a wide, sandy, multithreaded river | M, D, F | Dean and Schmidt 2013 |
| | | Scouring the channel bed of the river and offsetting the effects of sediment accumulation | M, D | Dean and Schmidt, 2011; Escobar-Arias and Pasternack, 2010 |
| | | Evacuates large quantities of fine sediment | M, D, R | Dean et al., 2016 |
| | | Morphodynamic changes of in-channel units and habitats | M, D, F | Wyrick and Pasternack, 2015; Weber and Pasternack, 2017 |
| | Biogeochemical | Addition of organic matter and nutrient flush | M, D | Nilsson and Malm 2008 |
| | | Respiration and soil carbon dynamics in riparian plants | M, T, F | Williams et al., 2006; Maier et al., 2011 |
| | | Increase turbidity and sedimentation | M, D, R | Nilsson and Malm 2008 |
| | | Restore water quality after prolongued low flows | M, D | Postel and Richter 2003 |
| | Biological | Flowering, fruting and seed dispersal | M, D, T | Simonin, 2000 |
| | | Drifting and dispersal of eggs and laevae | M, D, R | Humphries et al., 2020 |
| | | Reduction of predator density | M, D | Postel and Richter 2003 |
| Snowmelt flows | Physical | Scouring and sediment deposition | M, D | Happ 1948 |
| | | Overbank floodplain inundation | M, D, T, F | Stone et al., 2017 |
| | | recharge groundwater (floodplains) | M, D | Opperman et al 2017 |
| | Biogeochemical | Decrease water temperature | D, R | Stacey, N. E., 1984 |
| | | Increase export of nutrients and primary producers from floodplain to channel | M, D | Bowen et al. 2003, Ward and Stanford 1995 |
| | Biological | Provide hydrologic cues for fish outmigration and spawning; rearing | M,T,R | Yarnell et al 2020 |
| | | Seedling survival | M, R, D | Bhattacharjee(2006) |

The Big Bend Region illustrates the importance of annual and interannual floods. This region is an environmentally protected area, located downstream the confluence of the RGB mainstem and Rio Conchos, the main tributary. Before widespread human intervention altered the hydrology of the RGB, the Big Bend Region received two large pulses, one in spring and another one in summer or fall, similar in magnitude (Dean, 2021). In areas where the river flowed through valleys, flood pulses created multiple channels and sudden changes in its course. These pulses achieved several functions: they flushed sediments carried by tributaries; they controlled riparian vegetation, preventing the formation of floodplains; and they created wide channels with slow-moving water, which provided habitat for rearing and growth of native and endangered fish (Dean, 2021).

### 4.1.2 Impacts of changing the flood regime

Water diversions, reservoir operation and management, and river channelization have heavily altered the magnitude, frequency, duration, timing, and variability of high flows and floods throughout the basin, starting in the late 1800s (Blythe & Schmidt, 2018), but especially since the 1940s (Dean, 2021). As a result, many sections of the RGB have experienced channel narrowing and floodplain creation. In the Big Bend Region, this has resulted in a "laterally stable river with one channel and dense riverside vegetation", which reduces habitat for native and endangered species (Dean, 2021). Historic flood management, including river channelization and reservoir operation, and land-use change have caused increased flooding risk in human settlements adjacent to the river,

like the Presidio and Ojinaga communities, resulting in human, infrastructure, and economic losses. On some occasions, extreme, large floods have reset the river channel for brief periods (Dean, 2021).

### 4.1.3 Flood characterization

Several publications have addressed flood characteristics and ecological functions in the RGB. Dean and Schmidt have studied floods and geomorphic processes in the Big Bend Region. They have identified that, in the regulated hydrology, long duration floods with peaks larger than 1,000 m3/s have "eroded accumulated sediment, scour vegetation, and temporarily widen most of the channel", and thus are referred to as channel-resetting floods (Dean & Schmidt, 2013). Before the mid 1940s, these floods occurred once every five years, while from 1950 to 2012 there were only five flood events of this magnitude (1958, 1978, 1990, 1991, 2008) (Dean & Schmidt, 2013). After these floods, the channel narrowed, so between 1950 and 2008 the channel narrowed by more than 50% compared to pre-1950 channel width. In addition to the reduced magnitude and frequency of floods, the propagation of non-native vegetation since the 1900s has promoted channel narrowing. Vegetation stabilizes banks, increases channel margin roughness, and induces additional sediment deposition (Dean & Schmidt, 2013).

The flooding event that occurred in 2008 was studied (Dean & Schmidt, 2013). Discharge approached 1,500 $m^3/s$ and "breached levees, inundated communities, and flooded the alluvial valley of the Rio Grande; the wetted width exceeding 2.5 km in some locations." The river channel was narrow before the flood event and, after the flooding occurred,

the following geomorphic processes happened: channel widening, meander migration, avulsions, extensive bar formation, and vertical floodplain accretion.

Montero-Martinez and Ibañez-Hernandez (2017) studied flood events, amongst other environmental flows metrics, in the Rio Conchos Basin before and after the construction of a large dam, La Boquilla. They used regulated and naturalized streamflow data, the period of 1935 to 1950 corresponds to the natural hydrology, while the regulated hydrology encompasses from 1949 to 2014 (Montero-Martinez & Ibañez-Hernandez, 2017).

In natural hydrology, peak flows occurred in late August and early September, with an average magnitude of 180 $m^3/s$. However, in regulated hydrology, year-round streamflow experiences reductions from 65% to 99%, and peak flows occur from March to June and in September, with an average discharge of 2.25 $m^3/s$ (Montero-Martinez & Ibañez-Hernandez, 2017). The Natural Flow Regime components related to floods that experience alterations are peak flow magnitude and peak flow duration (Montero-Martinez & Ibañez-Hernandez, 2017). The main driver of change of the Natural Flow Regime is the Boquillas Dam, which serves hydropower, irrigation, and flood management objectives.

The World Wildlife Fund Mexico (2009) coordinated the estimation of environmental flows for nine locations in the Rio Conchos basin using the Building Block Method (World Wildlife Fund, 2009). The variables analyzed include hydrology, hydraulics,

hydrogeology, geomorphology, water quality, vegetation, fish and invertebrates. In relation to floods, peak flows were estimated for wet and dry years for each location. The recommended minima and maxima magnitudes in all stations range from 1 to 250 $m^3/s$ in dry years and from 5 to 500 $m^3/s$ in wet years. For each site, a reference hydrograph was recommended, which includes drought flows, maintenance flows, and average flows. In addition to considering ecological functions, these peak flow recommendations address flooding risk in communities located in the river floodplain.

Flood events occurring in the Northern branch of the RGB have also been studied (Blythe & Schmidt, 2018). After obtaining the daily naturalized streamflow with a mass-balance model in this portion of the basin, Blythe and Schmidt (2018) calculated several metrics of the annual peak flow, including magnitude and date, duration, and shape or symmetry. The period of record spans from 1900 to 2010.

The main findings include: magnitude, timing, and duration of floods decreased during the 20th century, with the greatest decreases occurring at the end of the century; the magnitude of regulated floods is 60% less than the natural floods; duration of floods is 20% shorter; timing was more variable, occurring later in the year compared to the natural floods (Blythe & Schmidt, 2018). Most remarkably, "the small floods of the estimated natural flow regime are now common floods, common floods of the estimated natural flow regime are now 20–50 year floods, and today, no floods occur during drought years" (Blythe & Schmidt, 2018).

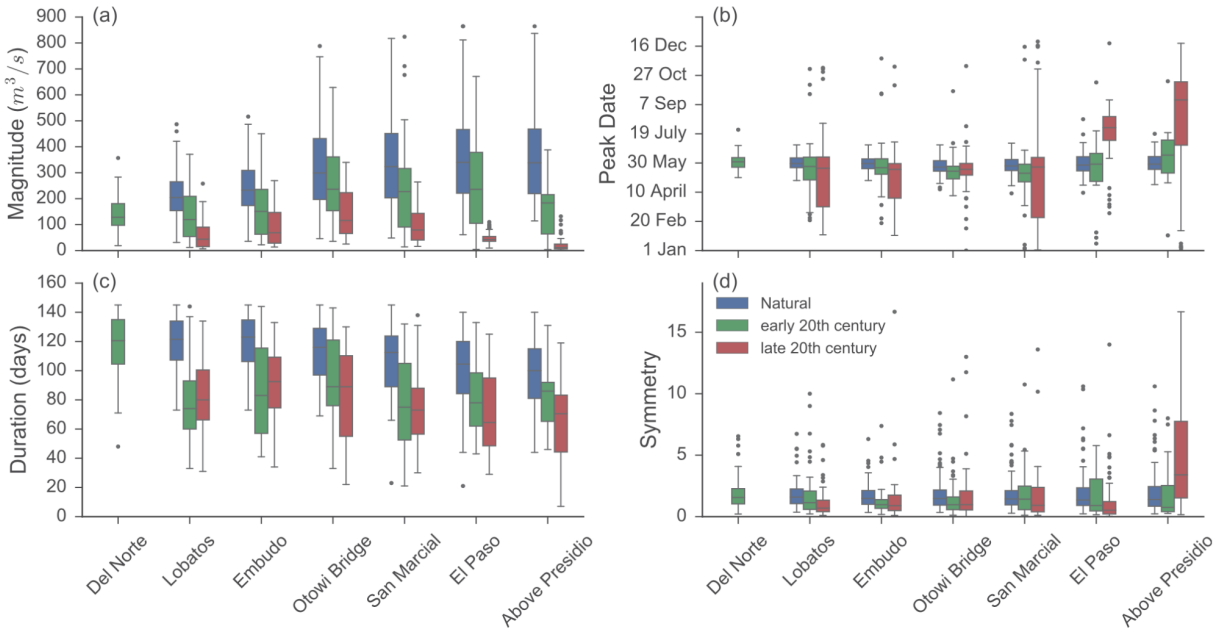


Figure 4. Flood characteristics in the Northern branch of the Rio Grande-Bravo (Blythe and Schmidt, 2018).

# 5 Results

## 5.1 Timing

At all Southern branch stations, the natural, median peak flow timing is between late August and early September, with very little variation between stations (Figure 5). At Rio Conchos, half of flood events are distributed between one month, from late August to late September. In the RGB Below Ojinaga and Foster Ranch, half of flood events are distributed between two months, from late July until late September. This changes at Amistad, Laredo, and Anzaldúas, half of flood events are distributed between three months, from late June until late September. Additionally, in these three stations the timing presents a bimodal distribution, which is incrementally marked in each subsequent downstream station.

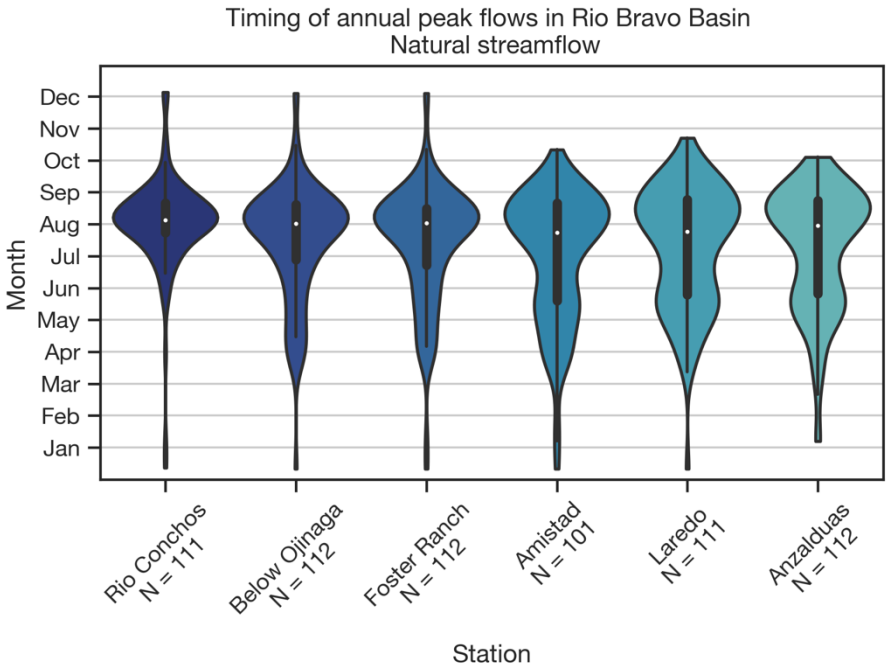


Figure 5. Timing of natural floods in the Southern branch of the RGB.

This corresponds with the natural flow regime in the Southern branch. The flow regime of the Rio Conchos is dominated by rainfall events caused, in most part, by the North American monsoon (Woodhouse et al., 2012), with additional flows resulting from tropical storms that either impact directly or approximate the Rio Conchos basin from both the Pacific and Atlantic Oceans (Sayto Corona et al., 2017). At downstream stations, particularly at Laredo and Anzaldúas, peak flow timing reflects the influence of two climatically-different headwaters (González-Escorcia, 2016): the snow-melt driven peaks that occur from late April to mid-June (Blythe & Schmidt, 2018) and the rainfall-dominated flows from Rio Conchos presented from late July to late September. Indeed, navigation reports reviewed by Blythe and Schmidt (2018) describe how annual high flows entered the Gulf of Mexico from April until August.

Figure 6 shows flood timing in four different time periods. The main differences between these four periods are several. First, some outlier values are found; several peak flows occur much earlier in the periods from 1930 to 1959 from Rio Conchos to Laredo, and in the period from 1990 to 2015, in Foster Ranch, Amistad, and Anzaldúas. Second, there is slightly more variation in the median between periods, especially in 1930-1959 and 1990-2015 in Amistad, Laredo, and Anzaldúas, with the median peak flow occurring up to a month earlier. Lastly, the bimodal distribution is not as marked in all periods; the interquartile range is much shorter in Amistad from 1960 to 1989, and at Laredo and Anzaldúas from 1990 to 2015. Otherwise, the values of median and the interquartile range are similar to the values of the 100-year timing timeseries.

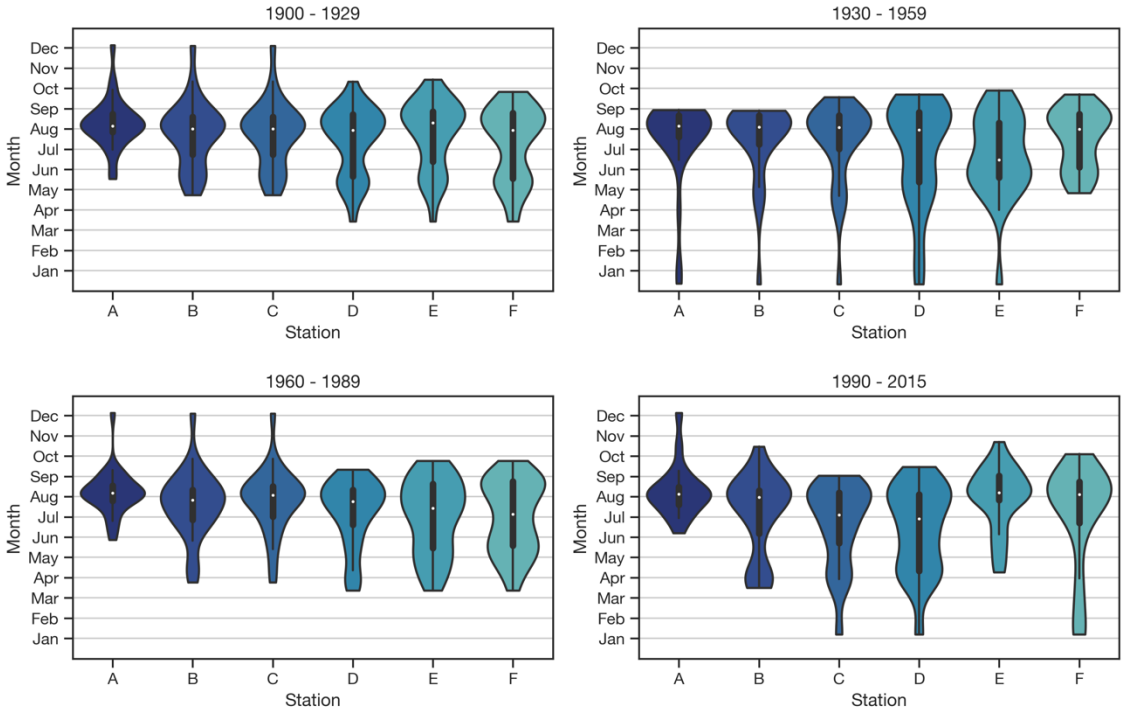


Figure 6. Timing of natural floods in the Southern branch of the RGB in different time periods. A: Rio Conchos, B: RGB below Ojinaga, C: RGB at Foster Ranch, D: RGB at Amistad, E: RGB at Laredo, F: RGB at Anzaldúas.

Figures 7 and 8 present peak flow timing of the regulated streamflow. The changes in timing between natural and regulated streamflow are discussed in the section “Change in timing.”

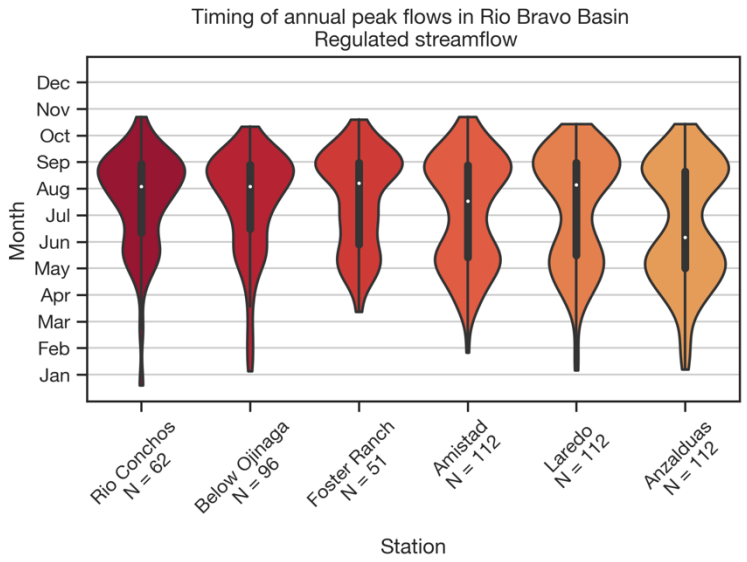


Figure 7. Timing of regulated floods in the Southern branch of the RGB.

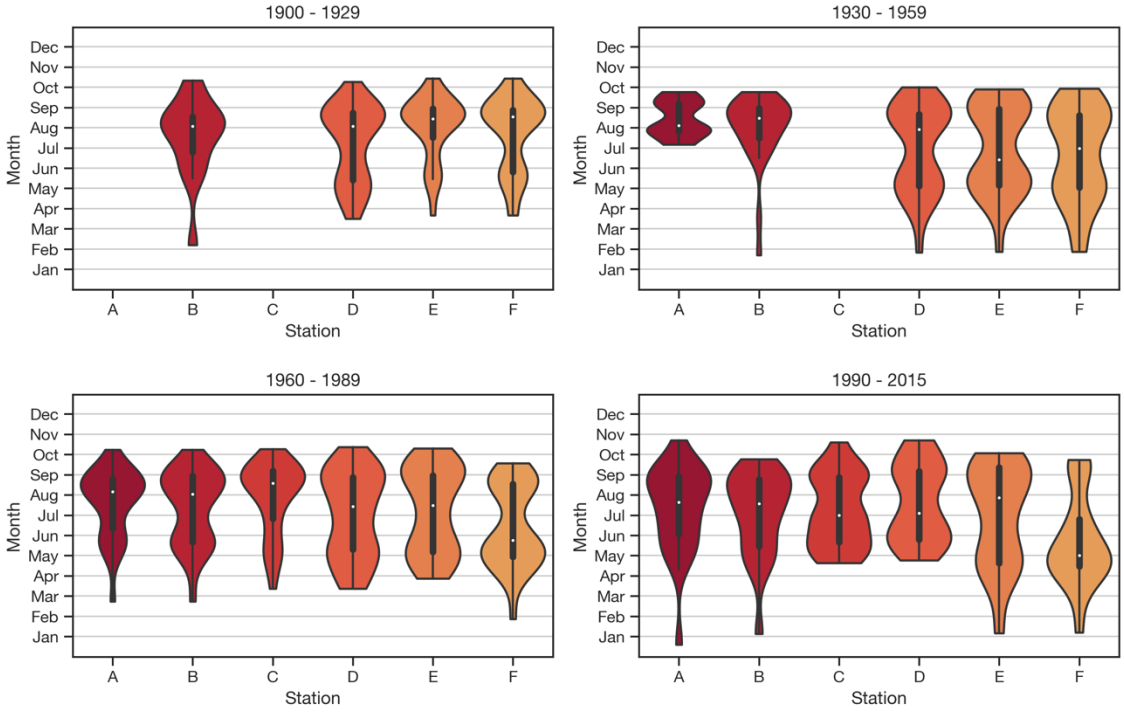


Figure 8. Timing of regulated floods in the Southern branch of the RGB in different time periods. A: Rio Conchos, B: RGB below Ojinaga, C: RGB at Foster Ranch, D: RGB at Amistad, E: RGB at Laredo, F: RGB at Anzaldúas.

## 5.2 Magnitude and frequency

### 5.2.1 Flood frequency analysis

Natural, median peak flow magnitude ranges from 720 $m^3/s$ at Rio Conchos to 2,250 $m^3/s$ in RGB at Anzaldúas. The minimum peak flow ranges from 59 to 440 $m^3/s$, while the maximum from 16,808 to 19,522 $m^3/s$. Downstream from Rio Conchos, in RGB below Ojinaga and at Foster Ranch, the median peak flow increases in increments of less than 10% in each station, while in downstream stations, RGB at Amistad, RGB at Laredo, and RGB at Anzaldúas, the median peak flow increases in increments from 20% to 35%.

In the regulated basin, median peak flow magnitude ranges from 199 $m^3/s$ at Rio Conchos to 648 $m^3/s$ in RGB at Anzaldúas, while the minimum ranges from 44 to 82 $m^3/s$, while the maximum from 1,490 to 7,203 $m^3/s$. The difference in the metrics of natural and regulated flows are outstanding; the median of regulated peak flows at the upstream and downstream stations decreases 70% (see Table 5), while minima and maxima at two stations show up to 90% reduction.

Table 5. Magnitude of natural and regulated floods in the Southern branch of the RGB.

| Annual peak flow magnitude ($m^3/s$) | | | | | | | | | |
|---|---|---|---|---|---|---|---|---|---|
| Metric | Rio Conchos | | | Below Ojinaga | | | Foster Ranch | | |
| | Natural | Regulated | Rel. change | Natural | Regulated | Rel. change | Natural | Regulated | Rel. change |
| **Minimum** | 59 | 44 | -26% | 200 | 14 | -93% | 202 | 70 | -66% |
| **Average** | 1,134 | 281 | -75% | 1,219 | 449 | -63% | 1,275 | 508 | -60% |
| **Median** | 720 | 199 | -72% | 799 | 251 | -69% | 837 | 306 | -63% |
| **Maximum** | 16,808 | 1,490 | -91% | 16,830 | 4,220 | -75% | 17,496 | 2,440 | -86% |
| **SD** | 1,707 | 315 | -82% | 1,689 | 591 | -65% | 1,741 | 548 | -69% |
| **IQR** | 889 | 140 | -84% | 906 | 346 | -62% | 957 | 401 | -58% |
| Metric | Amistad | | | Laredo | | | Anzaldúas | | |
| | Natural | Regulated | Rel. change | Natural | Regulated | Rel. change | Natural | Regulated | Rel. change |
| **Minimum** | 260 | 117 | -55% | 359 | 156 | -57% | 440 | 82 | -81% |
| **Average** | 1,812 | 1,406 | -22% | 2,296 | 1,500 | -35% | 3,181 | 1,225 | -61% |
| **Median** | 1,293 | 778 | -40% | 1,725 | 840 | -51% | 2,258 | 648 | -71% |
| **Maximum** | 17,516 | 11,672 | -33% | 19,479 | 16,300 | -16% | 19,522 | 7,023 | -64% |
| **SD** | 2,014 | 1,698 | -16% | 2,225 | 1,935 | -13% | 2,856 | 1,471 | -49% |
| **IQR** | 1,438 | 1,165 | -19% | 2,002 | 1,108 | -45% | 2,397 | 1,587 | -34% |

Figure 9 presents exceedance probability curves of peak flows at all stations, for natural and regulated streamflow. In the natural hydrology, above 60% probability of occurrence, peak flow magnitudes at Rio Conchos, RGB below Ojinaga, and RGB at Foster Ranch are very similar, while greater differences in magnitude can be observed between RGB at Amistad, Laredo, and Anzaldúas. Below 20% probability of occurrence, all stations, except for Rio Conchos, present peak flow magnitudes above 200 $m^3/s$. The curves of natural peak flows barely overlap below 90% of occurrence, which shows that

peak flows of all magnitudes increase proportionally as the river travels downstream, which is expected in the natural hydrology of the basin.

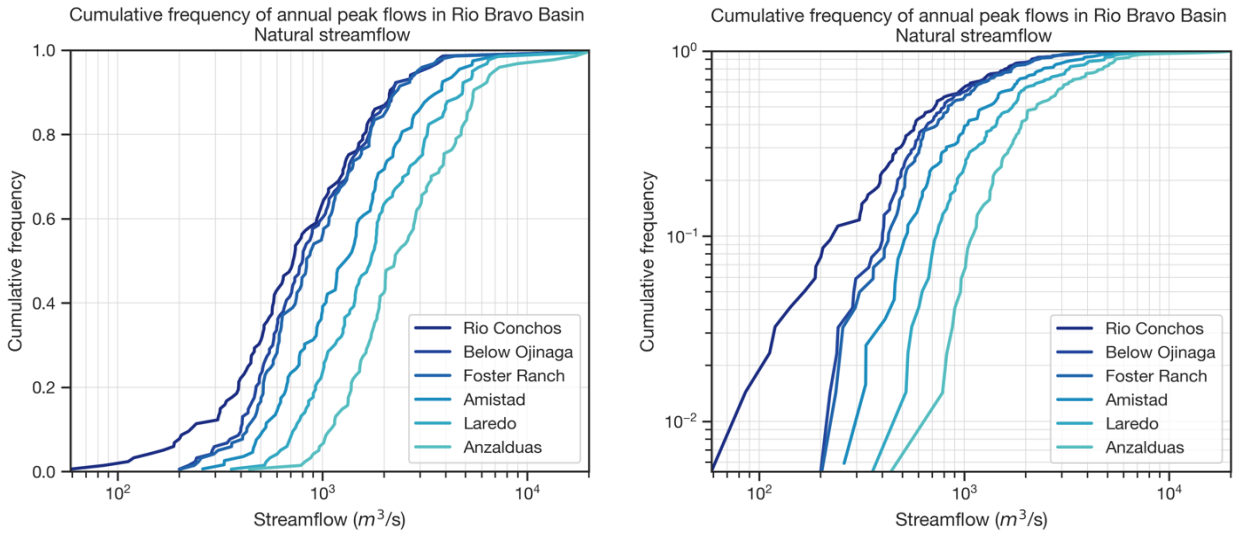


Figure 9. Exceedance probability curves of the natural flood events. Left figure: horizontal axis with logarithmic scale. Right: horizontal and vertical axis with logarithmic scale.

In contrast, the curves of the regulated peak flows overlap. For instance, below 70% of occurrence in RGB at Amistad and Laredo, peak flow magnitudes are larger than in RGB at Anzaldúas, which is located downstream from these two stations. Similarly, below 20% of occurrence in RGB below Ojinaga, peak flows fall below 40 $m^3/s$, while Rio Conchos, located upstream from RGB below Ojinaga, experiences peak flows of at least 40 $m^3/s$. This illustrates how peak flow magnitude does not increase proportionally as the river travels downstream, they are now influenced by the operation of reservoirs.

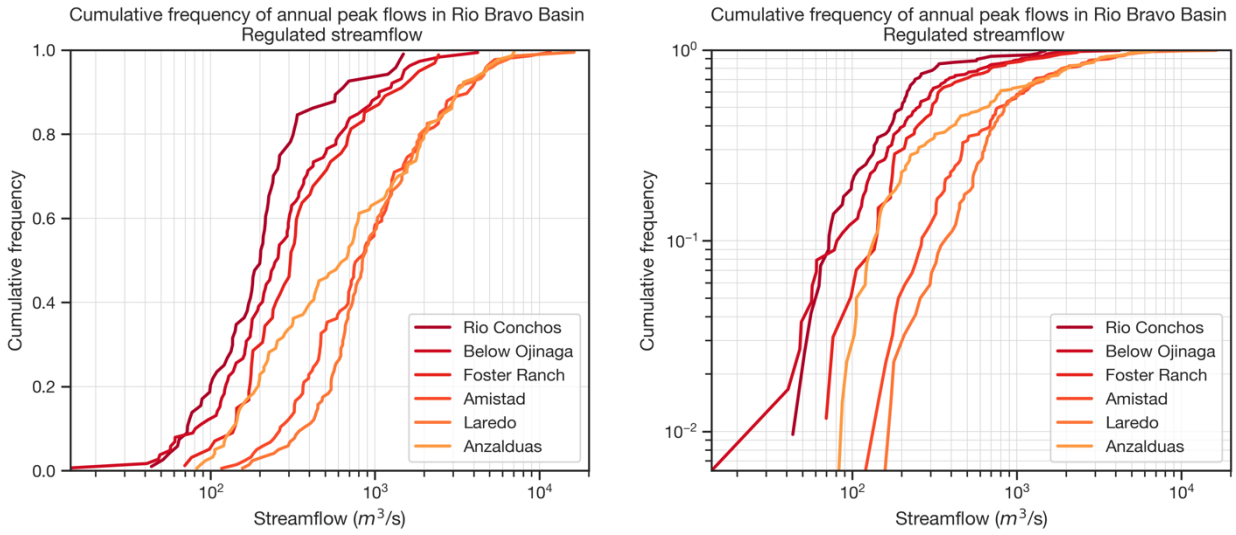


Figure 10. Exceedance probability curves of the regulated flood events. Left figure: horizontal axis with logarithmic scale. Right: horizontal and vertical axis with logarithmic scale.

Table 5 presents metrics of the natural and regulated peak flows. Median peak flow magnitude presents significant decreases, above 60%, at Rio Conchos, at RGB below Ojinaga, at Foster Ranch, and Anzaldúas. Rio Conchos is the station where most metrics show the largest difference between natural and regulated peak flows, while Amistad is the station with the smallest difference. This is presented visually in Figure 11, which compares the exceedance probability curves of natural and regulated hydrology in each station. Most notably, at RGB in Anzaldúas, there is a significant difference in natural and regulated magnitudes below 70% probability of occurrence.

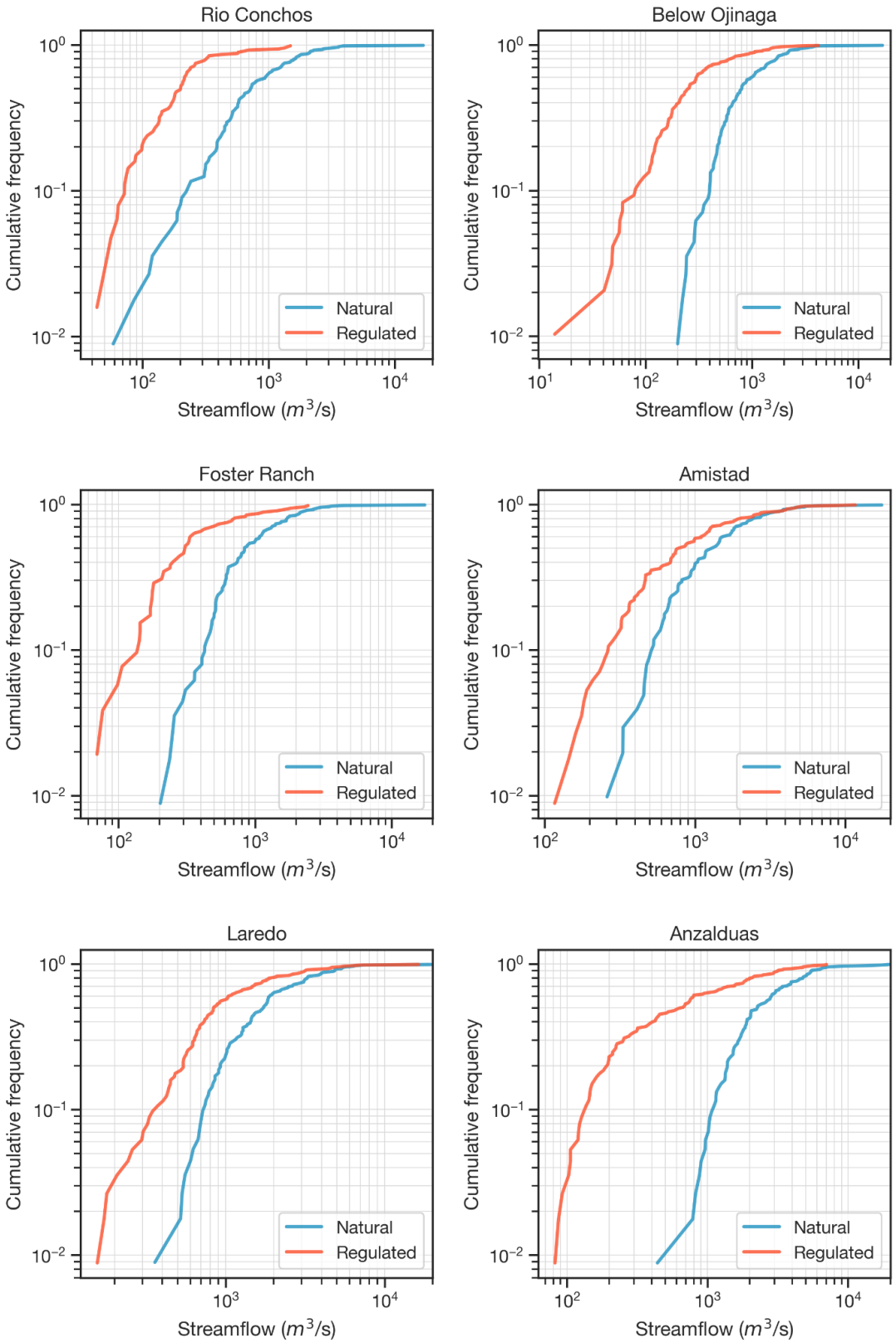


Figure 11. Exceedance probability curves of the natural and regulated floods, with both axis in a logarithmic scale.

### 5.2.2 Flood magnitude prediction

Table 6 presents the median magnitude of estimated annual peak flows of different return periods: 2, 5 and 10 years, which correspond to the 50th, 80th and 90th percentiles, respectively. Estimated magnitudes were obtained using the 110-year time series in windows of 20 years and the cumulative distribution function of the LP3 fitting shown in Figures 21, 22, 23 and 24 (supplemental materials). In natural hydrology, the 2-year peak flow estimate ranges from 750 $m^3/s$ at Rio Conchos to 2,372 $m^3/s$ in RGB at Anzaldúas, while the 10-year estimate ranges from 2,055 $m^3/s$ to 6,083 $m^3/s$. In the regulated hydrology, the 2-year peak flow estimate ranges from 179 $m^3/s$ at Rio Conchos to 616 $m^3/s$ in RGB at Anzaldúas, while the 10-year estimate ranges from 576 $m^3/s$ to 3,002 $m^3/s$. The largest changes in the median between natural and regulated hydrology are observed in Rio Conchos, at RGB below Ojinaga, RGB at Foster Ranch, and RGB at Anzaldúas, where the relative change ranges from 50% to 76%.

Figures 12, 13, and 14 show the estimated annual peak flows for natural and regulated streamflow from 1900 to 2010. Regarding the 10-year magnitude estimate, from 1920 to 2000, in Rio Conchos, RGB below Ojinaga, and RGB at Foster Ranch, there is little variation in peak flow magnitudes, ranging from 1,500 $m^3/s$ to 3,000 $m^3/s$. However, in RGB at Laredo and RGB at Anzaldúas, magnitude estimates present larger changes across time. In RGB at Laredo, from 1920 to 1960 magnitudes range from 4,000 to 6,000 $m^3/s$, decreasing to below 4,000 $m^3/s$ after 1960. In RGB at Anzaldúas, from 1920 to 1960

magnitudes range from 4,000 to 8,000 $m^3/s$, with the lowest values occurring in 1940, this pattern is repeated from 1960 to 2000, with the lowest values occurring in 1980.

Table 6. Natural and regulated estimated flood magnitudes for 2-, 5- and 10-year return periods.

| Estimated peak flow magnitude ($m^3/s$) | | | | | | | | | |
|---|---|---|---|---|---|---|---|---|---|
| Metric | Rio Conchos | | | Below Ojinaga | | | Foster Ranch | | |
| | Natural | Regulated | Rel. change | Natural | Regulated | Rel. change | Natural | Regulated | Rel. change |
| **Median (observed)** | 720 | 199 | -72% | 799 | 251 | -69% | 837 | 306 | -63% |
| **T = 2** | 758 | 179 | -76% | 833 | 264 | -68% | 893 | 316 | -65% |
| **T = 5** | 1,482 | 360 | -76% | 1,508 | 619 | -59% | 1,582 | 693 | -56% |
| **T = 10** | 2,055 | 576 | -72% | 2,072 | 948 | -54% | 2,141 | 1,074 | -50% |
| | | | | | | | | | |
| Metric | Amistad | | | Laredo | | | Anzaldúas | | |
| | Natural | Regulated | Rel. change | Natural | Regulated | Rel. change | Natural | Regulated | Rel. change |
| **Median (observed)** | 1,293 | 778 | -40% | 1,725 | 840 | -51% | 2,258 | 648 | -71% |
| **T = 2** | 1,283 | 838 | -35% | 1,700 | 931 | -45% | 2,372 | 616 | -74% |
| **T = 5** | 2,336 | 1,945 | -17% | 2,996 | 2,006 | -33% | 4,334 | 1,733 | -60% |
| **T = 10** | 3,224 | 3,082 | -4% | 4,069 | 3,097 | -24% | 6,083 | 3,002 | -51% |

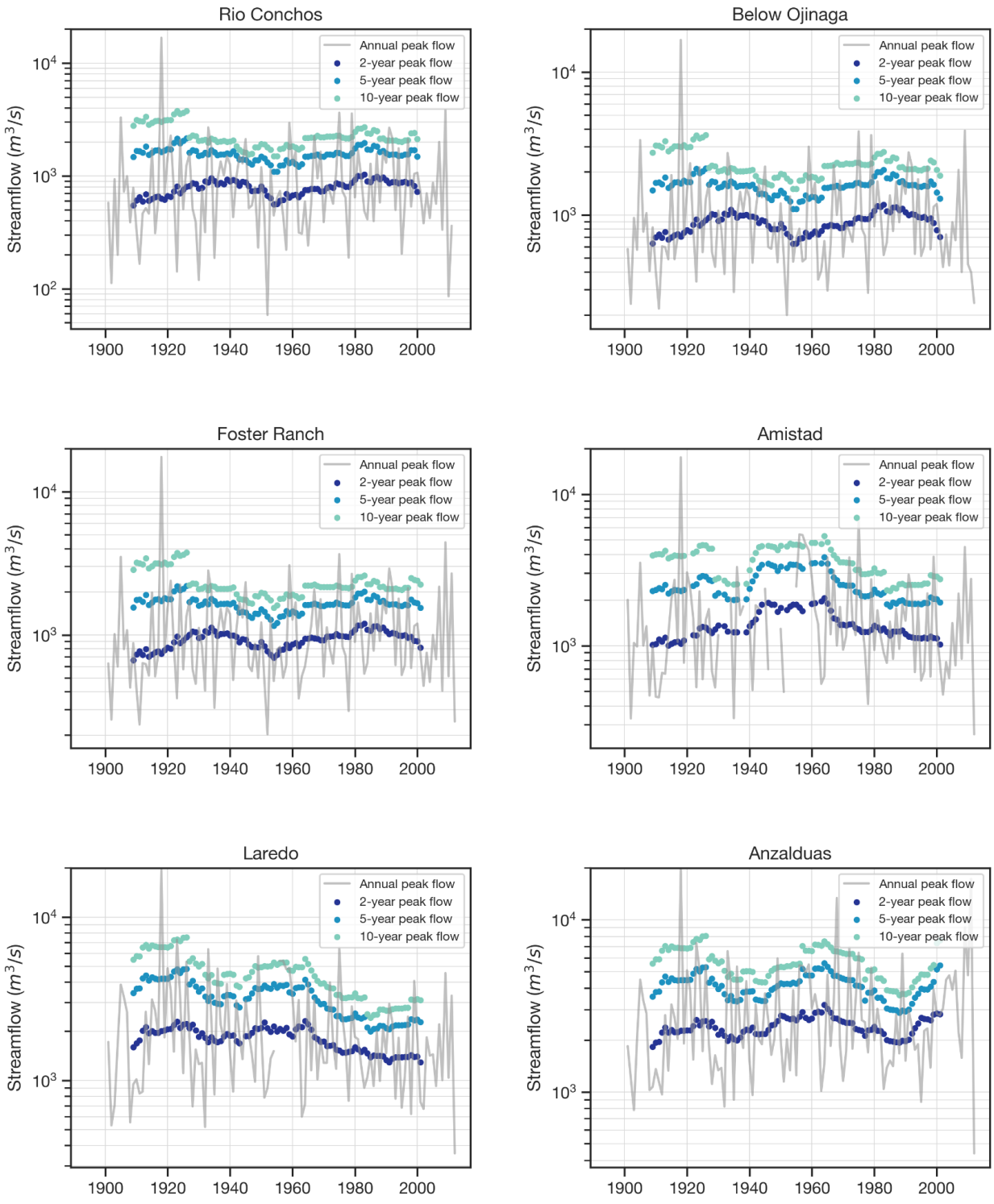


Figure 12. Estimated 2-, 5- and 10-year flood magnitude for natural streamflow.

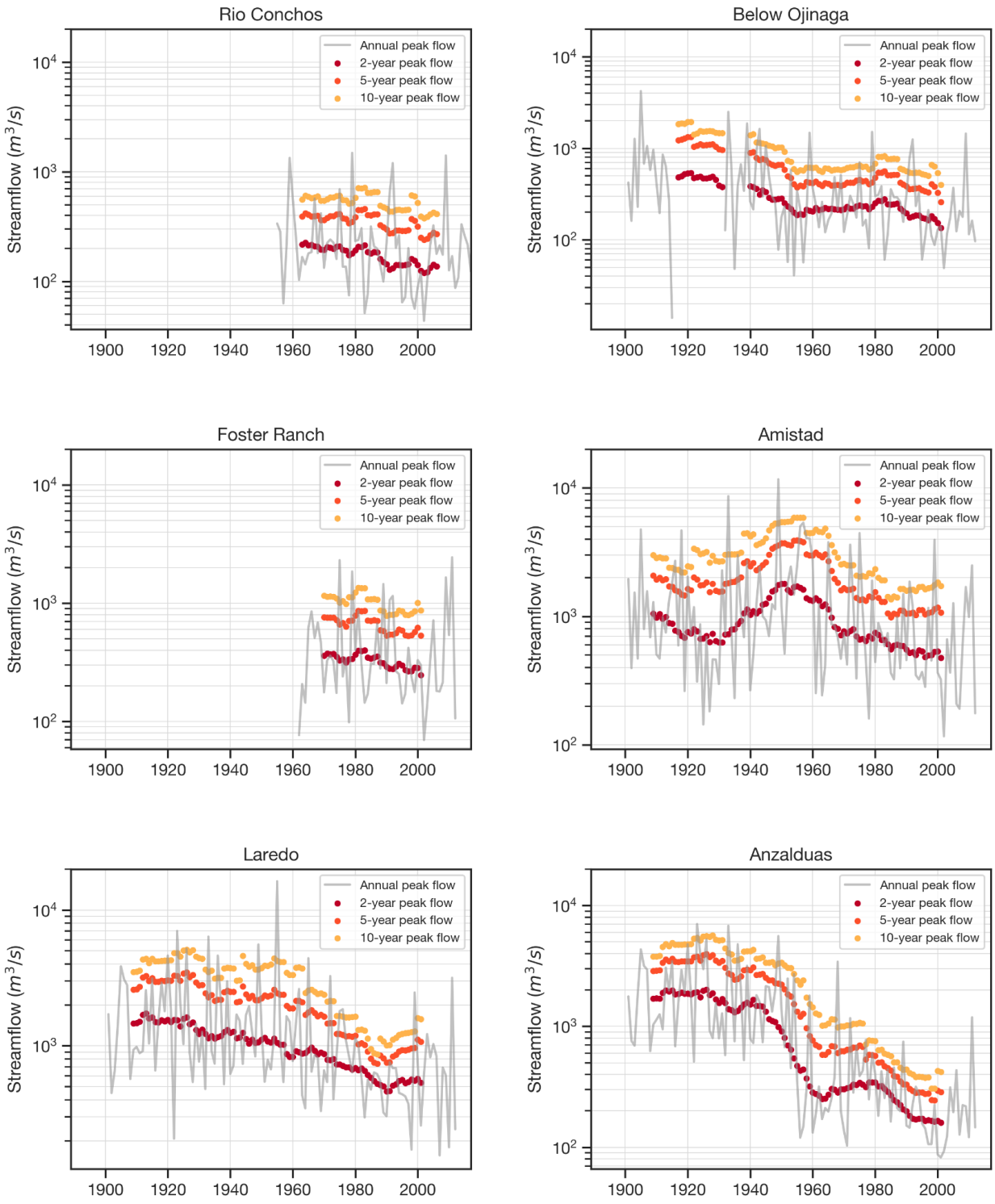


Figure 13. Estimated 2-, 5- and 10-year flood magnitude for regulated streamflow.

Changes between natural and regulated 10-year magnitude estimates across time are more noticeable at RGB below Ojinaga, RGB at Laredo, and RGB at Anzaldúas, where regulated streamflow records are longer. In RGB below Ojinaga and RGB at Anzaldúas, there is a marked decrease in estimated regulated peak flows from 1940 onwards, with Anzaldúas presenting the starkest differences between natural and regulated floods. in RGB at Laredo, regulated floods start decreasing from 1960.

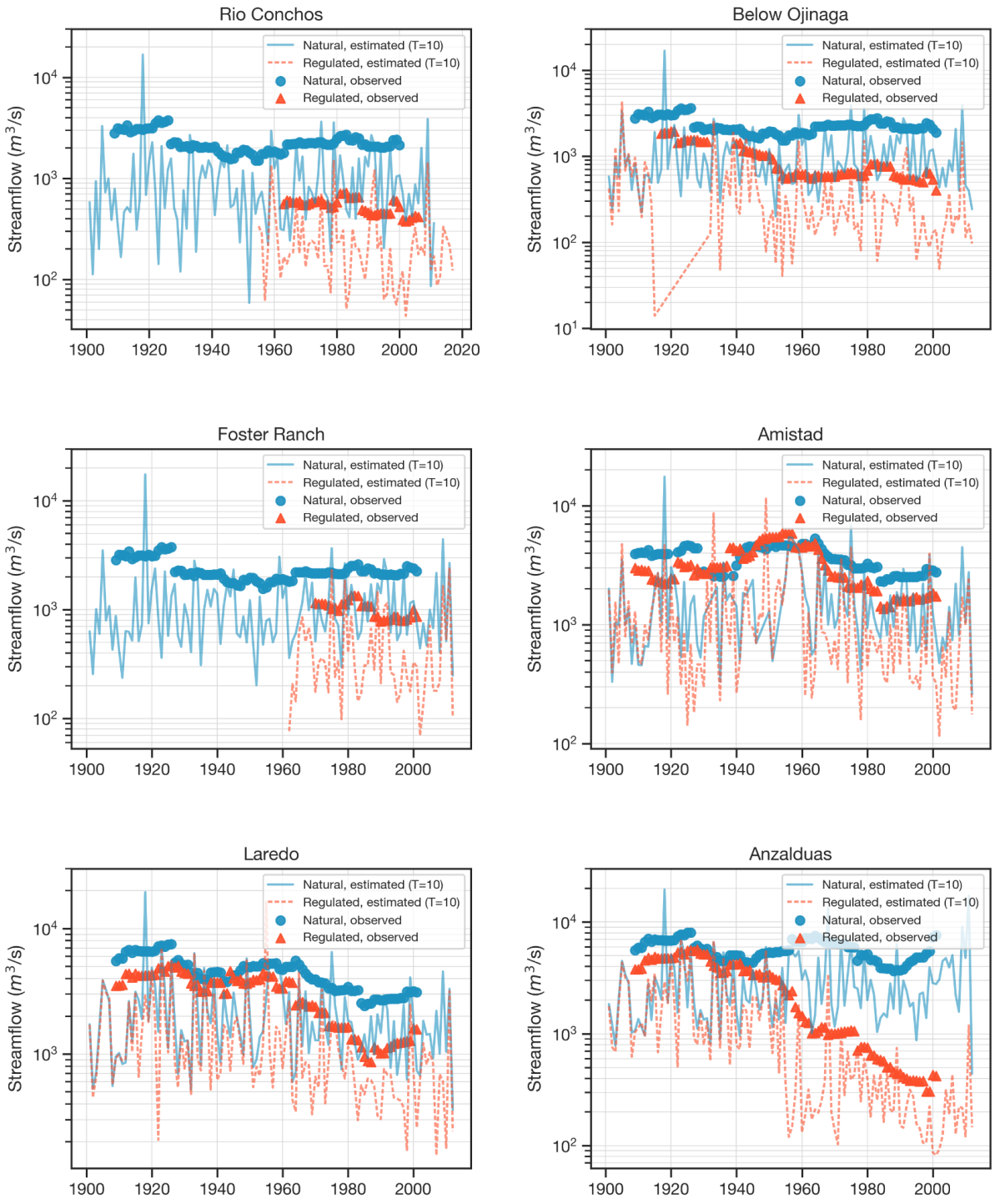


Figure 14. Estimated 2-, 5- and 10-year flood magnitude for natural and regulated streamflow.

## 5.3 Comparison of natural and regulated floods

### 5.3.1 Change in timing

At all stations except RGB at Anzaldúas, regulated median peak flows occur within 14 days in relation to the natural median peak flows. In RGB at Anzaldúas, median peak flows occur over two months earlier. At Rio Conchos and RGB at Foster Ranch, the IQR is larger compared to the natural timing; half of flood events occur within almost two months and over three months, respectively, instead of one month and two months. At Rio Conchos, in RGB below Ojinaga, and in RGB at Foster Ranch, maximum peak flows occur between 1.5 months and 2 months earlier in the year.

Table 7. Comparison of natural and regulated peak flow timing metrics.

| Annual peak flow timing | | | | | | | | | |
|---|---|---|---|---|---|---|---|---|---|
| Metric | Rio Conchos | | | Below Ojinaga | | | Foster Ranch | | |
| | Natural | Regulated | Difference (days) | Natural | Regulated | Difference (days) | Natural | Regulated | Difference (days) |
| **Minimum** | Jan 11 | Jan 18 | 7 | Jan 10 | Feb 3 | 24 | Jan 10 | Apr 11 | 91 |
| **Average** | Aug 29 | Aug 15 | -13 | Aug 13 | Aug 13 | 0 | Aug 11 | Aug 16 | 5 |
| **Median** | Sep 1 | Aug 30 | -2 | Aug 28 | Aug 30 | 2 | Aug 29 | Sep 3 | 5 |
| **Maximum** | Dec 30 | Nov 17 | -43 | Dec 29 | Nov 6 | -53 | Dec 29 | Nov 14 | -45 |
| **SD** | 45 | 56 | 11 | 53 | 57 | 4 | 55 | 55 | 0 |
| **IQR** | 28 | 78 | 50 | 52 | 73 | 21 | 54 | 93 | 39 |

| Metric | Amistad | | | Laredo | | | Anzaldúas | | |
|---|---|---|---|---|---|---|---|---|---|
| | Natural | Regulated | Difference (days) | Natural | Regulated | Difference (days) | Natural | Regulated | Difference (days) |
| **Minimum** | Jan 10 | Feb 24 | 45 | Jan 10 | Feb 4 | 25 | Feb 5 | Feb 5 | 0 |
| **Average** | Jul 29 | Aug 3 | 4 | Aug 7 | Aug 6 | 0 | Aug 5 | Jul 19 | -17 |

| Annual peak flow timing | | | | | | | | | |
|---|---|---|---|---|---|---|---|---|---|
| Metric | Rio Conchos | | | Below Ojinaga | | | Foster Ranch | | |
| | Natural | Regulated | Difference (days) | Natural | Regulated | Difference (days) | Natural | Regulated | Difference (days) |
| **Median** | Aug 20 | Aug 14 | -6 | Aug 21 | Sep 1 | 12 | Aug 26 | Jul 4 | -54 |
| **Maximum** | Nov 6 | Nov 17 | 11 | Nov 17 | Nov 9 | -8 | Oct 30 | Nov 9 | 10 |
| **SD** | 61 | 61 | 1 | 56 | 64 | 7 | 57 | 66 | 9 |
| **IQR** | 92 | 104 | 12 | 90 | 105 | 15 | 88 | 110 | 22 |

Figure 15 presents the violin plots of both natural and regulated peak flows. Compared to the natural peak flows, all stations in the regulated hydrology present two periods of peak flows, one between late spring and early summer, and another one between late summer and early fall. In contrast, the natural peak flows, especially at Rio Conchos, RGB below Ojinaga, and RGB at Foster Ranch, concentrate between late summer and early fall. This bimodal distribution is more marked in the downstream stations. Even though in RGB at Anzaldúas the median peak flow occurs much earlier, it maintains the bimodal distribution.

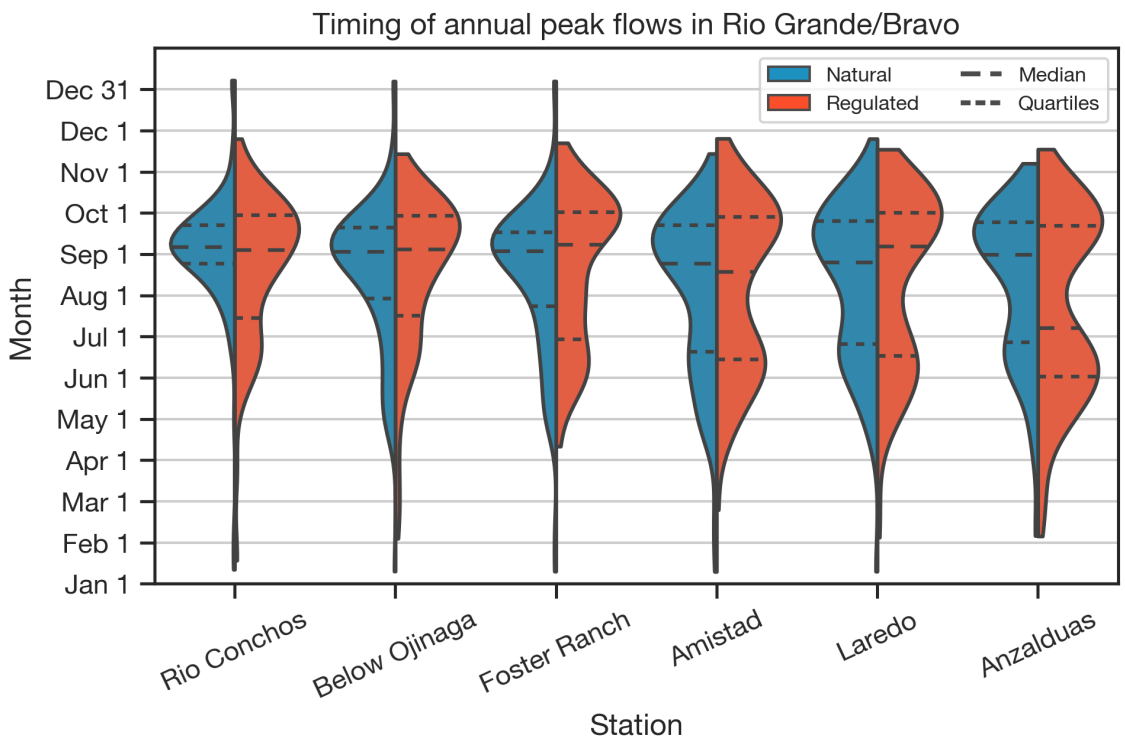


Figure 15. Violin plots comparing natural and regulated peak flow timing.

### 5.3.2 Change in magnitude

Index 1 describes how peak flow magnitude has changed over time. It compares the 10-year estimated natural and 10-year estimated regulated peak flows, dividing the regulated estimate by the natural estimate. The question this index seeks to answer is: what is the proportion between the regulated and the natural flood magnitude estimate for a given year? In other words, how small or big is the regulated flood magnitude when compared to the natural flood magnitude. For example, an Index 1 of 0.5 means that the regulated flood magnitude is 50% of the natural flood magnitude, and index of 1 means that the regulated and natural flood magnitudes are the same, and an Index 1 greater than 1 means that the regulated flood magnitudes are larger than in the natural flow regime.

At all stations except RGB at Amistad, the proportion between regulated and natural floods is less than 1.0, meaning the regulated flood magnitude is smaller in the regulated regime than in the natural flow regime. At stations with more data availability, RGB below Ojinaga, RGB at Laredo, and RGB at Anzaldúas, Index 1 has values above 0.5 before 1960, which means that the magnitude of regulated peak flows represent around 50% of the natural peak flows. However, after the 1960s, Index 1 decreased, most notably in RGB at Anzaldúas, where it ranged around 0.25 until the 1990s, and dropped to less than 0.15 by the 2000s. This indicates that regulated peak flows represent around 25% and 15% of the natural peak flows. In RGB at Amistad, Index 1 reached values higher than 1.0, up to 1.75, between 1930 and 1960. This means that the magnitude of regulated floods is larger than that of natural floods, which might be due to the operation of Amistad Dam in the regulated hydrology during those 30 years. In Rio Conchos and RGB at Foster Ranch, Index 1 has values around 0.25 and 0.5, respectively, from 1960 and 1970 onwards.

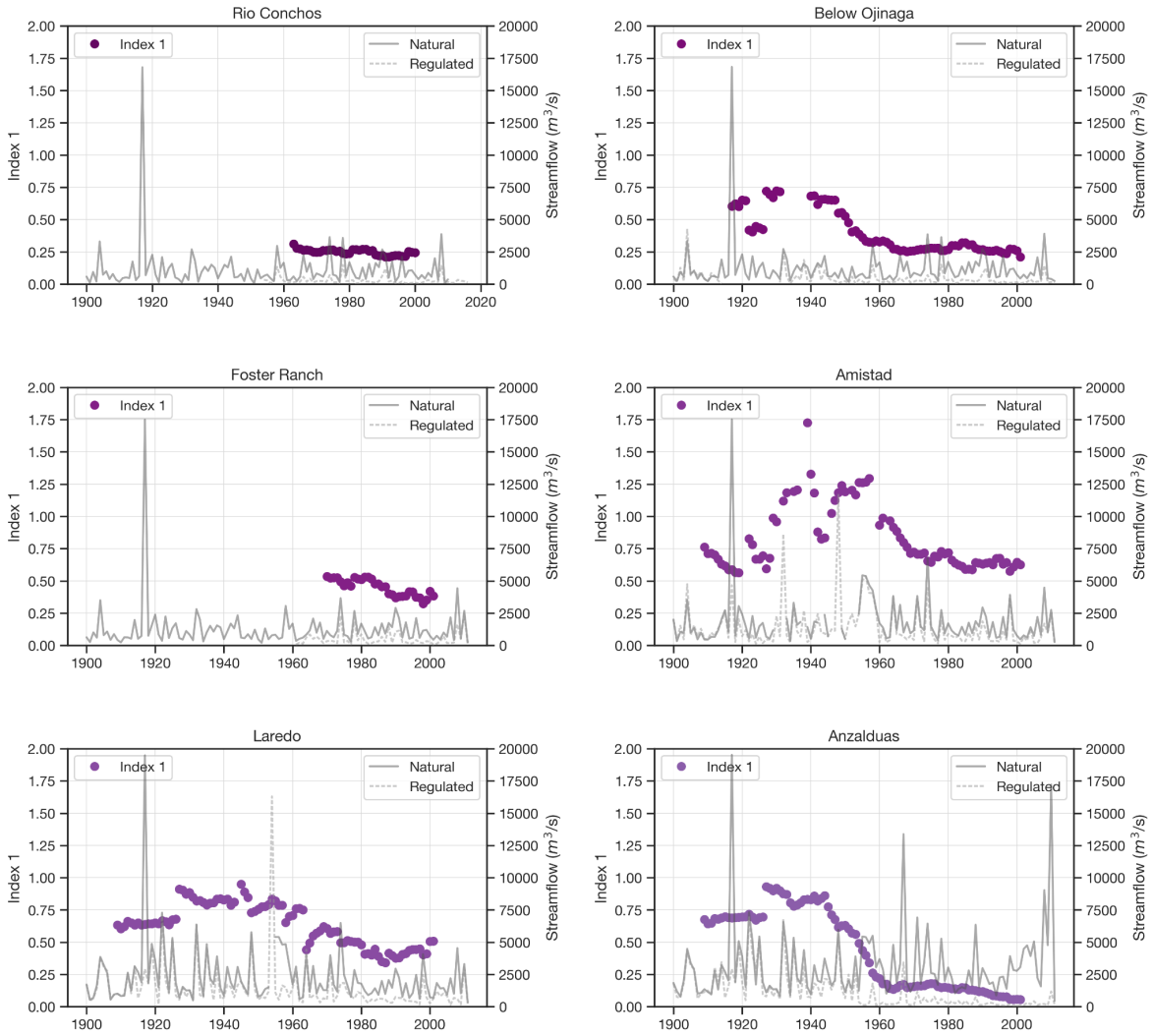


Figure 16. Index 1, which compares the estimated magnitude of natural and regulated floods.

### 5.3.3 Change in frequency

Index 2 presents the frequency with which the magnitude of 10-year natural floods occur in the regulated hydrology. The questions this index seeks to answer are: how often do natural flood magnitudes occur in the regulated hydrology and how does this frequency compare to the frequency of natural floods? For example, an Index 2 with a value of 5 means that a given flow in the regulated streamflow used to occur 5 times more often in the natural regime.

At stations with more data availability, RGB below Ojinaga, RGB at Laredo, RGB at Amistad, and RGB at Anzaldúas, Index 2 has values below 2, with some values under 1, before 1960, which means that the frequency with which 10-year natural floods would have occurred is roughly the same or twice as often as that of regulated floods. After 1960, these stations presented values over 2 and up to 5 in RGB at Laredo and up to 7 in RGB at Anzaldúas. This means that the frequency with which 10-year natural floods occur is up to 5 or 7 times the frequency of regulated flows. In other words, a 10-year flood in the natural regime now takes seven times more time (70 years) to occur in the regulated streamflow regime. In RGB at Laredo and RGB at Anzaldúas, floods with magnitudes comparable to the natural hydrology do not occur with the same frequency. In Rio Conchos and RGB at Foster Ranch, Index 2 has values below 2 from 1960 onwards.

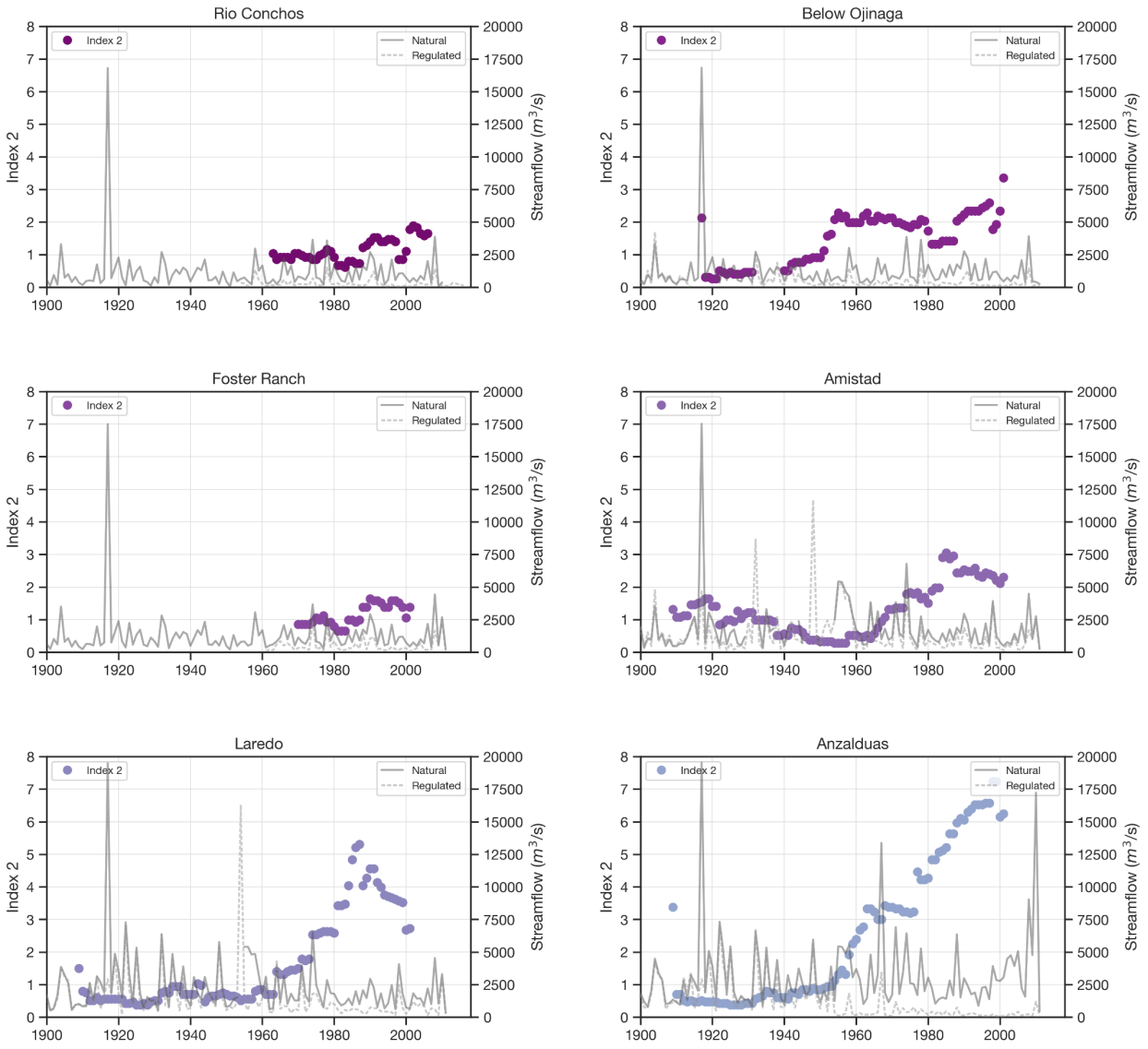


Figure 17. Index 2, which compares the frequency of natural and regulated floods.

# 6 Discussion and conclusions

## 6.1 Discussion

Peak flow timing, magnitude, and frequency have significant implications for physical (Figure 18), biogeochemical, and biological (Figure 19) ecosystem functions. The life stages of several species are timed with peak floods, while physical and biogeochemical functions triggered by floods of a certain magnitude and frequency support habitat creation and maintenance. It is important to note that flood functions work synergistically: flood timing cannot be isolated from other components like flood magnitude or frequency. For example, for floods to support fish migration they should occur during late spring, with an annual frequency, and a certain magnitude to create a river corridor.

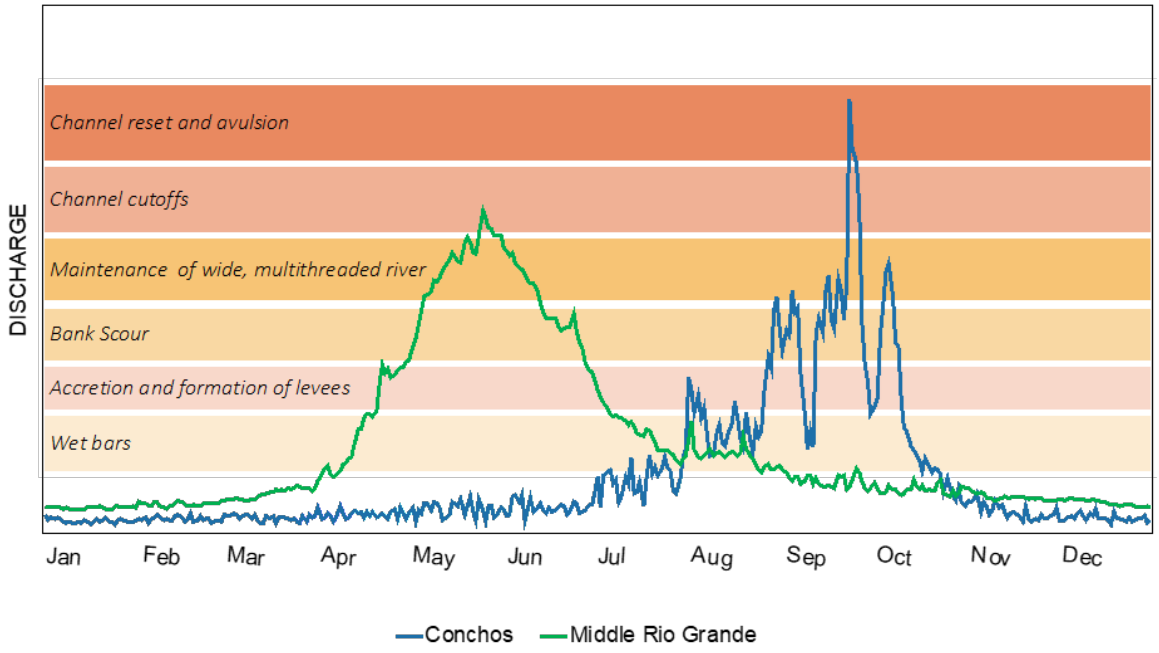


Figure 18. Physical functions of the natural flow regime of the Rio Conchos and the Middle Rio Grande (Garza-Díaz, 2022).

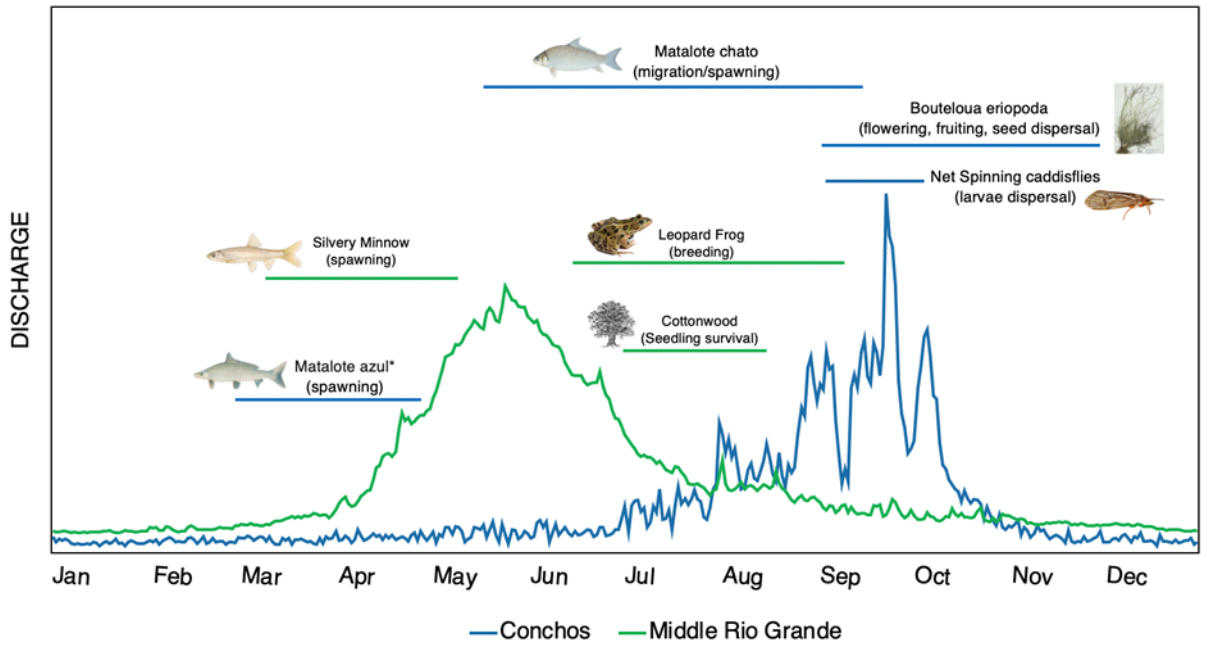


Figure 19. Biological functions of the natural flow regime of the Rio Conchos and the Middle Rio Grande (Garza-Díaz, 2022).

The following are ecosystem functions where flood timing is a significant component at the Southern branch, compiled by Garza-Díaz (2022). Snowmelt floods, occurring in spring and early summer, cause overbank floodplain inundation and provide cues for fish migration and spawning. Likewise, summer pulse flows, occurring in July, provide cues for fish migration and support conditions for spawning. Monsoon peak flows, presented from August until mid-October, increase soil microbial response and flux of carbon and nitrogen pools, and support growing periods for riparian plants. Lastly, wet season high flows, which encompass the functional flows mentioned earlier, support respiration and soil carbon dynamics in riparian plants and flowering and seed dispersal.

These ecological functions are affected by the following changes in timing. The station located closest to the basin outlet, RGB at Anzaldúas, experiences the most significant changes in timing, with median peak flows occurring up to two months earlier, in July instead of September. This has implications for estuary health. In the regulated hydrology, all stations present a bimodal distribution, which means that less floods occur in late summer and, instead, occur in late spring, especially in Rio Conchos, RGB below Ojinaga, RGB at Foster Ranch, and RGB at Amistad. This means snowmelt floods are more frequent compared to the natural hydrology, while monsoon peak flows are less common. Lastly, the distribution of half of flood events is longer in Rio Conchos and RGB at Foster Ranch, with a higher incidence of summer pulses in Rio Conchos, and more frequent summer pulses and snowmelt floods in RGB at Foster Ranch.

The following are ecosystem functions where flood magnitude and frequency play a significant role at the Southern branch, compiled by Garza-Díaz (2022). Summer pulse flows trigger sediment deposition, construction of levees, bank scouring, and egg aeration in spawning sites. Monsoon peak flows support channel reset, avulsion, and braiding, meander migration, and cutoffs. Wet season high flows maintain a wide, sandy, and multithreaded river, and trigger morphodynamic changes of in-channel units and habitats. Some additional functions where magnitude is a relevant component are the following: summer pulse flows modify salinity conditions in estuaries; monsoon peak flows deposit nutrients in floodplains, remove generalists and support survival of native species; wet season high flows scour the channel bed of the river, offset the effects of sediment accumulation, add organic matter and flush nutrients, increase turbidity and sedimentation, restore water quality, and reduce predator density; lastly, snowmelt flows support scouring, sediment deposition, and seedling survival.

The main changes in flood magnitude and frequency are the following. The median of regulated flood magnitudes decreased down to 70% in four stations: Rio Conchos, RGB below Ojinaga, RGB at Foster Ranch, and RGB at Anzaldúas. The most remarkable difference between the natural and the regulated hydrology is that the largest floods occur in two stations located upstream the river outlet, RGB at Amistad and RGB at Laredo. This is opposite to natural hydrology, where the largest floods in the basin should occur downstream. Changes between natural and regulated 10-year magnitude estimates across time are more noticeable at RGB below Ojinaga, RGB at Laredo, and

RGB at Anzaldúas. In RGB below Ojinaga and RGB at Anzaldúas, there is a marked decrease in estimated regulated peak flows from 1940 onwards, with Anzaldúas presenting the starkest differences between natural and regulated floods. in RGB at Laredo, regulated floods start decreasing from 1960.

The changes in magnitude and frequency are well documented in existing literature. With fewer, smaller floods there is less sediment transport, which translates into stable banks and a narrower, incised channel with dense vegetation which, in turn, prevent the river from braiding and meandering, obstructing the formation of pools, riffles, and runs. This means there are less flood events with the capacity to reset the river channel and restore the shallow and wide channel. Additionally, the lack of periodic, large floods provides less opportunities to flush the river channel and reset water quality.

There are at least two groups of studies in the Southern branch of the RGB that make environmental flows recommendations, including flood timing, magnitude, and frequency, informed by ecological restoration and water management goals. As mentioned earlier, the World Wildlife Fund Mexico made environmental flows recommendations for nine locations in the Rio Conchos. The recommended minima and maxima magnitudes in all stations range from 1 to 250 $m^3/s$ in dry years and from 5 to 500 $m^3/s$ in wet years. A reference hydrograph was obtained for each site, which includes drought flows, maintenance flows, and average flows. In addition to considering ecological functions, these peak flow recommendations address flooding risk in communities located in the river floodplain.

Sandoval-Solis and McKinney (2014) estimated the maximum volume of environmental flows that can be allocated in the Big Bend Region without compromising human water management goals, including water demand and flooding risk in communities. It was estimated that large floods with return periods between one and three years can occur from July to December, with magnitudes ranging from 45 $m^3/s$ to 102 $m^3/s$, with the largest floods occurring in August and October. The following is an annual hydrograph estimated for the Big Bend Reach (Sandoval-Solis & McKinney, 2014).

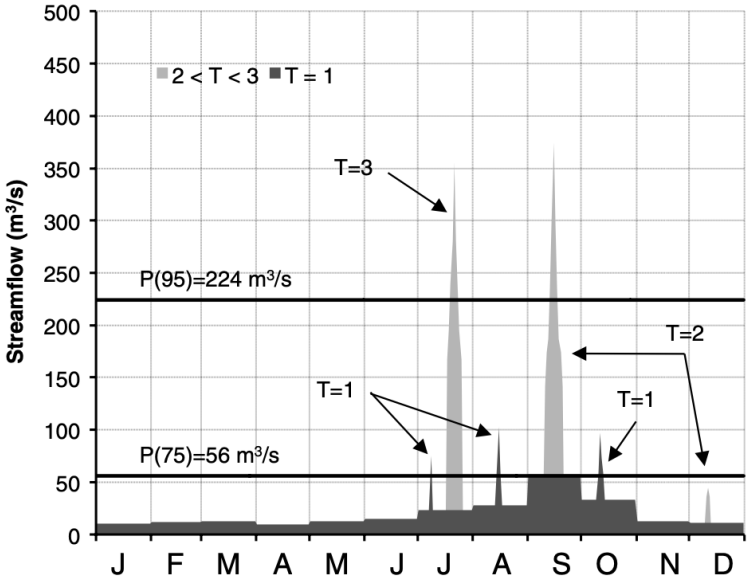


Figure 20. Recommended annual hydrograph to maximize ecologic and human water management goals at the Big Bend Region (Sandoval-Solis & McKinney, 2014).

## 6.2 Conclusion

It is possible to estimate flood characteristics, particularly timing, magnitude, and frequency, using daily natural and regulated streamflow data. This data can be used to make a quantitative comparison between flood events in a natural and regulated flow regime. Additionally, a temporal analysis of changes in magnitude and frequency can

help understand climatic variability in a basin, understanding streamflow as a proxy for climate.

The main findings of this research are: (1) natural flood timing reflects the climatic drivers of two main headwaters: flood events during the snowmelt season in the northern branch above Presidio/Ojinaga, and during the monsoon season in the southern branch; (2) in the regulated regime, floods occur earlier in the year, most notably at the basin outlet; (3) natural median floods range from 720 $m^3/s$ at the headwaters to 2,250 $m^3/s$ at the basin outlet; (4) regulated median flood magnitudes decrease 70% in four stations, with larger floods occurring in stations located upstream the river outlet, opposite to natural hydrology; (5) the 10-year natural flood estimates range from 2,055 $m^3/s$ to 6,083 $m^3/s$; (6) natural flood estimates show a pattern of dry and wet periods; and (7) frequency of large floods decrease at all stations, most noticeably after 1960.

Changes in flood timing, magnitude, and frequency have significant implications for physical, biogeochemical, and biological ecosystem functions. The life stages of several species are timed with floods, like fish spawning and migration. Physical and biogeochemical functions triggered by predictable, large floods support habitat creation by regulating water quality, preventing channel narrowing, depositing nutrients in the floodplain, and clearing out invasive species, amongst many other functions. Water management alternatives to reproduce functional flows, especially floods, have already

been proposed by several authors, showing it is possible to restore ecological functions and satisfy human water management goals.

# 7 References


Arthington, A. H. (2012). *Environmental Flows: Saving Rivers in the Third Millennium*. University of California Press. https://doi.org/10.1525/california/9780520273696.001.0001

Arthington, A. H., & Balcombe, S. R. (2011). Extreme flow variability and the 'boom and bust' ecology of fish in arid-zone floodplain rivers: A case history with implications for environmental flows, conservation and management. *Ecohydrology*, *4*(5), 708–720. https://doi.org/10.1002/eco.221

Balcombe, S. R., Bunn, S. E., Arthington, A. H., Fawcett, J. H., Mckenzie-Smith, F. J., & Wright, A. (2007). Fish larvae, growth and biomass relationships in an Australian arid zone river: Links between floodplains and waterholes. *Freshwater Biology*, *52*(12), 2385–2398. https://doi.org/10.1111/j.1365-2427.2007.01855.x

Bastos, A., Naipal, V., Ahlström, A., MacBean, N., Smith, W., & Poulter, B. (2022). *Semiarid ecosystems* (pp. 311–335). https://doi.org/10.1016/B978-0-12-814952-2.00012-5

Beck, H. E., Zimmermann, N. E., McVicar, T. R., Vergopolan, N., Berg, A., & Wood, E. F. (2018). Present and future Köppen-Geiger climate classification maps at 1-km resolution. *Scientific Data*, *5*(1), Article 1. https://doi.org/10.1038/sdata.2018.214

Bilbe, L. (2006). *Anthropomorphic Effects on the Rio Grande: A Biogeographic Assessment* (p. 81). Texas State University. https://www.meadowscenter.txst.edu/rio/Biogeographic%20Assessment%20of%20the%20Rio%20Grande%206.pdf

Blythe, T. L., & Schmidt, J. C. (2018). Estimating the Natural Flow Regime of Rivers With Long-Standing Development: The Northern Branch of the Rio Grande. *Water Resources Research*, *54*(2), 1212–1236. https://doi.org/10.1002/2017WR021919

Bobée, B., Cavadias, G., Ashkar, F., Bernier, J., & Rasmussen, P. (1993). Towards a systematic approach to comparing distributions used in flood frequency analysis. *Journal of Hydrology*, *142*(1), 121–136. https://doi.org/10.1016/0022-1694(93)90008-W

Bunn, S. E., Thoms, M. C., Hamilton, S. K., & Capon, S. J. (2006). Flow variability in dryland rivers: Boom, bust and the bits in between. *River Research and*

*Applications*, *22*(2), 179–186. https://doi.org/10.1002/rra.904

Dadson, S. J., Lopez, H. P., Peng, J., & Vora, S. (2019). Hydroclimatic Extremes and Climate Change. In S. J. Dadson, D. E. Garrick, E. C. Penning-Rowsell, J. W. Hall, R. Hope, & J. Hughes (Eds.), *Water Science, Policy, and Management* (1st ed., pp. 11–28). Wiley. https://doi.org/10.1002/9781119520627.ch2

Dean, D. J. (2021). A river of change—The Rio Grande in the Big Bend region. In *A river of change—The Rio Grande in the Big Bend region* (USGS Numbered Series No. 2021–3036; Fact Sheet, Vols. 2021–3036, p. 4). U.S. Geological Survey. https://doi.org/10.3133/fs20213036

Dean, D. J., & Schmidt, J. C. (2013). The geomorphic effectiveness of a large flood on the Rio Grande in the Big Bend region: Insights on geomorphic controls and post-flood geomorphic response. *Geomorphology*, *201*, 183–198. https://doi.org/10.1016/j.geomorph.2013.06.020

England, J. F., Jr., Cohn, T. A., Faber, B. A., Stendiger, J. R., Thomas, W. O., Jr., Veilleux, A. G., Kiang, J. E., & Mason, R. R., Jr. (2018). Guidelines for determining flood flow frequency—Bulletin 17C (ver. 1.1, May 2019). In *U.S. Geological Survey Techniques and Methods: Vol. Chapter B5* (p. 148). https://doi.org/10.3133/tm4B5.

Garza-Díaz, L. E. (2022). *A Quantitative Framework on Ecological Resilience for River Basins. Case Study: The Rio Grande – Rio Bravo*. University of California, Davis.

González-Escorcia, Y. A. (2016). *Determinación del caudal natural en la cuenca transfronteriza del Río Bravo/Grande* [Instituto Politécnico Nacional]. http://watermanagement.ucdavis.edu/files/8715/5424/5317/Gonzalez-Escorcia_201_Natural_Flow_Rio_Grande-Bravo_-_Thesis.pdf

Haktanir, T., & Horlacher, H. B. (1993). Evaluation of various distributions for flood frequency analysis. *Hydrological Sciences Journal*, *38*(1), 15–32. https://doi.org/10.1080/02626669309492637

Helsel, D. R., Hirsch, R. M., Ryberg, K. R., Archfield, S. A., & Gilroy, E. J. (2020). Statistical methods in water resources. In *Statistical methods in water resources* (USGS Numbered Series No. 4-A3; Techniques and Methods, Vols. 4-A3, p. 484). U.S. Geological Survey. https://doi.org/10.3133/tm4A3

Hernández, A., Martin-Puertas, C., Moffa-Sánchez, P., Moreno-Chamarro, E., Ortega, P., Blockley, S., Cobb, K. M., Comas-Bru, L., Giralt, S., Goosse, H., Luterbacher, J.,

Martrat, B., Muscheler, R., Parnell, A., Pla-Rabes, S., Sjolte, J., Scaife, A. A., Swingedouw, D., Wise, E., & Xu, G. (2020). Modes of climate variability: Synthesis and review of proxy-based reconstructions through the Holocene. *Earth-Science Reviews, 209*, 103286. https://doi.org/10.1016/j.earscirev.2020.103286

Hewlett, J. D. (1982). *Principles of Forest Hydrology*. University of Georgia Press.

Interagency Advisory Committee on Water Data. (1982). *Guidelines for determining flood flow frequency—Bulletin 17B*. U.S. Geological Survey. https://water.usgs.gov/osw/bulletin17b/dl_flow.pdf

Kidson, R., & Richards, K. S. (2005). Flood frequency analysis: Assumptions and alternatives. *Progress in Physical Geography: Earth and Environment*, *29*(3), 392–410. https://doi.org/10.1191/0309133305pp454ra

Mimikou, M. A., Baltas, E. A., & Tsihrintzis, V. A. (2016). *Hydrology and Water Resource Systems Analysis* (0 ed.). CRC Press. https://doi.org/10.1201/9781315374246

Montero-Martinez, M. J., & Ibañez-Hernandez, O. F. (2017). *La cuenca del río Conchos: Una mirada desde las ciencias ante el cambio climático*. Instituto Mexicano de Tecnología del Agua.

Parasiewicz, P., King, E. L., Webb, J. A., Piniewski, M., Comoglio, C., Wolter, C., Buijse, A. D., Bjerklie, D., Vezza, P., Melcher, A., & Suska, K. (2019). The role of floods and droughts on riverine ecosystems under a changing climate. *Fisheries Management and Ecology, 26*(6), 461–473. https://doi.org/10.1111/fme.12388

Poff, N. L., Allan, J. D., Bain, M. B., Karr, J. R., Prestegaard, K. L., Richter, B. D., Sparks, R. E., & Stromberg, J. C. (1997). The Natural Flow Regime. *BioScience*, *47*(11), 769–784. https://doi.org/10.2307/1313099

Sandoval-Solis, S., & McKinney, D. C. (2014). Integrated Water Management for Environmental Flows in the Rio Grande. *Journal of Water Resources Planning and Management*, *140*(3), 355–364. https://doi.org/10.1061/(ASCE)WR.1943-5452.0000331

Sandoval-Solis, S., Paladino, S., Garza-Diaz, L., Nava, L., Friedman, J., Ortiz-Partida, J. P., Plassin, S., Gomez-Quiroga, G., Koch, J., Fleming, J., Lane, B., Wineland, S., Mirchi, A., Saiz-Rodriguez, R., & Neeson, T. (2022). Environmental flows in the Rio Grande—Rio Bravo basin. *Ecology and Society, 27*(1). https://doi.org/10.5751/ES-12944-270120

Sayto Corona, D., Silva Hidalgo, H., Sandoval-Solis, S., Álvarez Herrera, C., & Herrera Peraza, E. (2017). Aproximación e impacto directo de ciclones tropicales a la cuenca del río Conchos, Chihuahua, México. *Investigación y Cienca de La Universidad Autónoma de Aguascalientes*, *25*(72), 53–61.

Scholes, R. J. (2020). The Future of Semi-Arid Regions: A Weak Fabric Unravels. *Climate*, *8*(3), Article 3. https://doi.org/10.3390/cli8030043

Stedinger, J., & Foufoula-Georgiou, E. (1993). Frequency Analysis of Extreme Events. *Handbook of Hydrology*, *18*.

Teegavarapu, R. S. V., Salas, J. D., & Stedinger, J. R. (2019). *Statistical Analysis of Hydrologic Variables*. American Society of Civil Engineers. https://doi.org/10.1061/9780784415177

Walker, K. F., Sheldon, F., & Puckridge, J. T. (1995). A perspective on dryland river ecosystems. *Regulated Rivers: Research & Management*, *11*(1), 85–104. https://doi.org/10.1002/rrr.3450110108

Watson, I., & Burnett, A. D. (2017). *Hydrology: An Environmental Approach*. Routledge. https://doi.org/10.1201/9780203751442

Woodhouse, C., Stahle, D., & Villanueva Díaz, J. (2012). Rio Grande and Rio Conchos water supply variability over the past 500 years. *Climate Research*, *51*(2), 147–158. https://doi.org/10.3354/cr01059

World Wildlife Fund. (2009). *Propuesta de caudal ecológico en la cuenca del río Conchos y su consideración en el estudio de disponibilidad de aguas superficiales*. WWF Mexico.

Yarnell, S. M., Petts, G. E., Schmidt, J. C., Whipple, A. A., Beller, E. E., Dahm, C. N., Goodwin, P., & Viers, J. H. (2015). Functional Flows in Modified Riverscapes: Hydrographs, Habitats and Opportunities. *BioScience*, *65*(10), 963–972. https://doi.org/10.1093/biosci/biv102

# Supplemental materials

## Flood magnitude prediction: distribution fitting

Overall, the LP3 function proved a good fit to the annual peak flow data, both for the natural and the regulated streamflow records. Figures 21 and 22 show the Quantile-quantile plots and Probability Plot Correlation Coefficient of the natural and regulated peak flow data series fit to the LP3 distribution function. Figures 23 and 24 present the cumulative distribution function of the LP3 fit and the 110-year annual peak flow data with 5% and 95% confidence intervals.

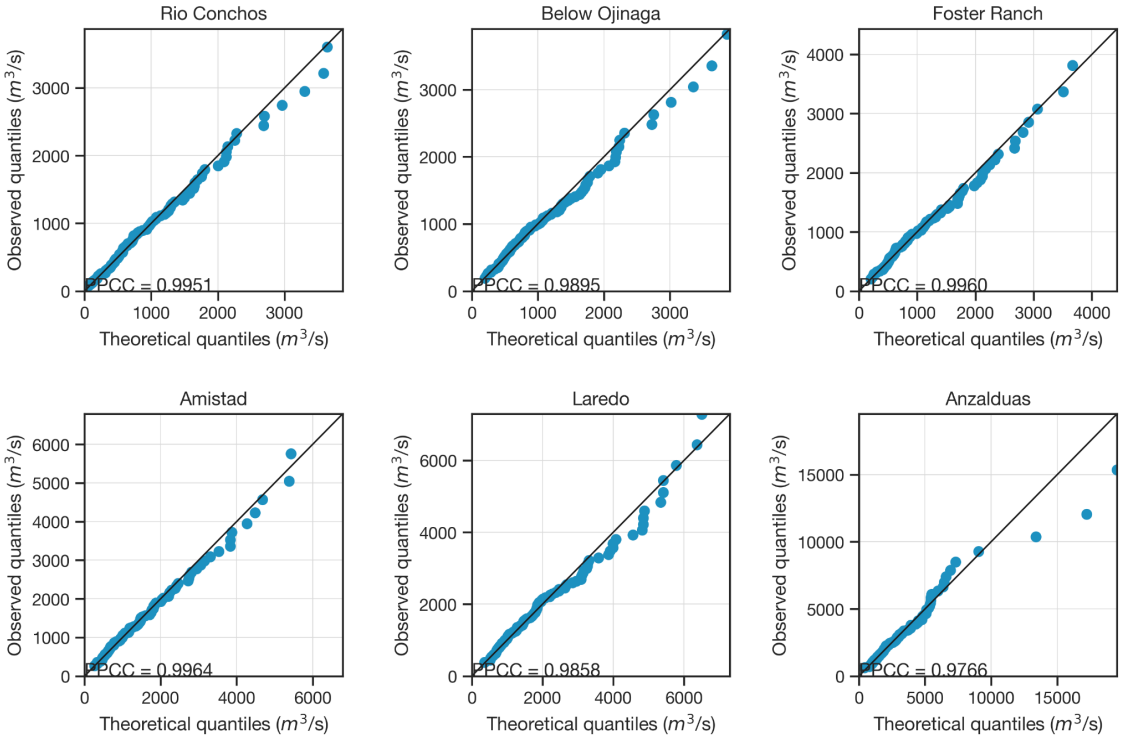


Figure 21. Quantile-quantile plots and Probability Plot Correlation Coefficient of the natural peak flow data series to the LP3 distribution function.

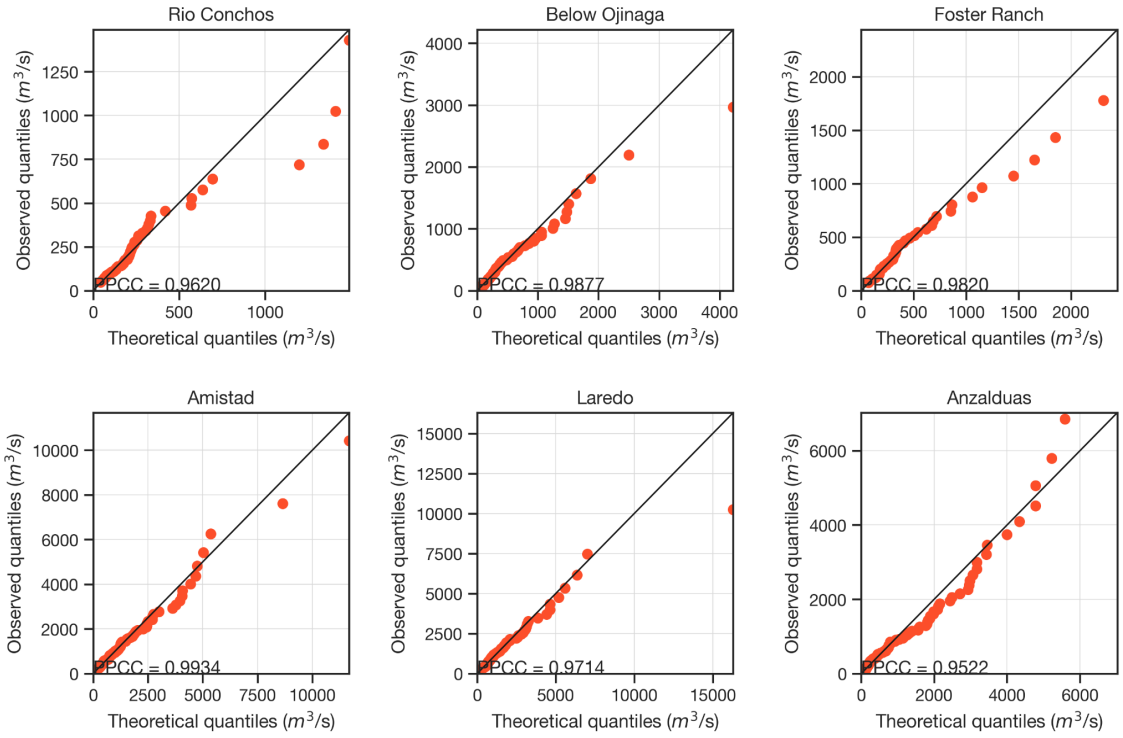


Figure 22. Quantile-quantile plots and Probability Plot Correlation Coefficient of the regulated peak flow data series to the LP3 distribution function.

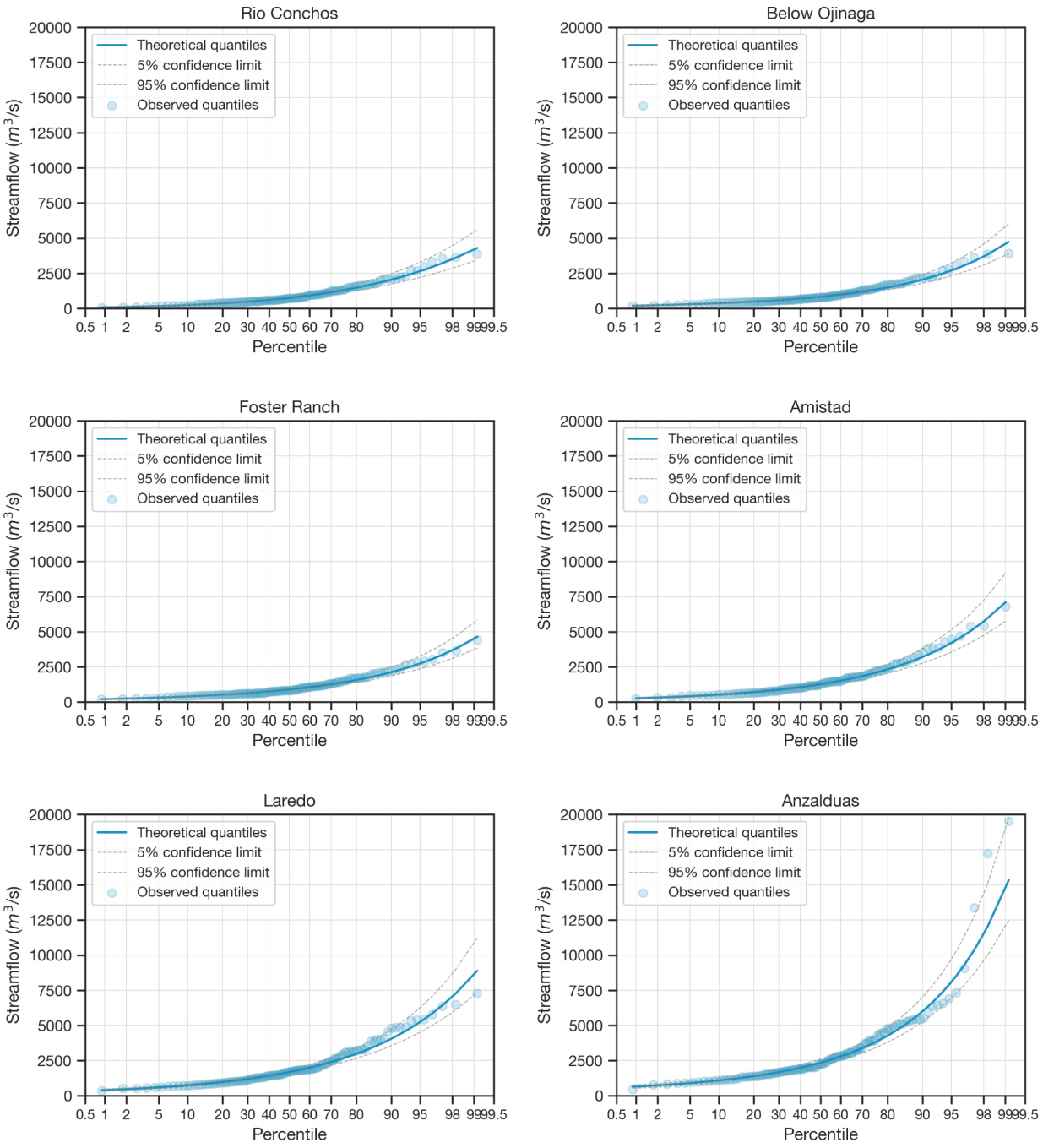


Figure 23. Probability plots with 5% and 95% confidence intervals of the natural peak flow data series to the LP3 distribution function.

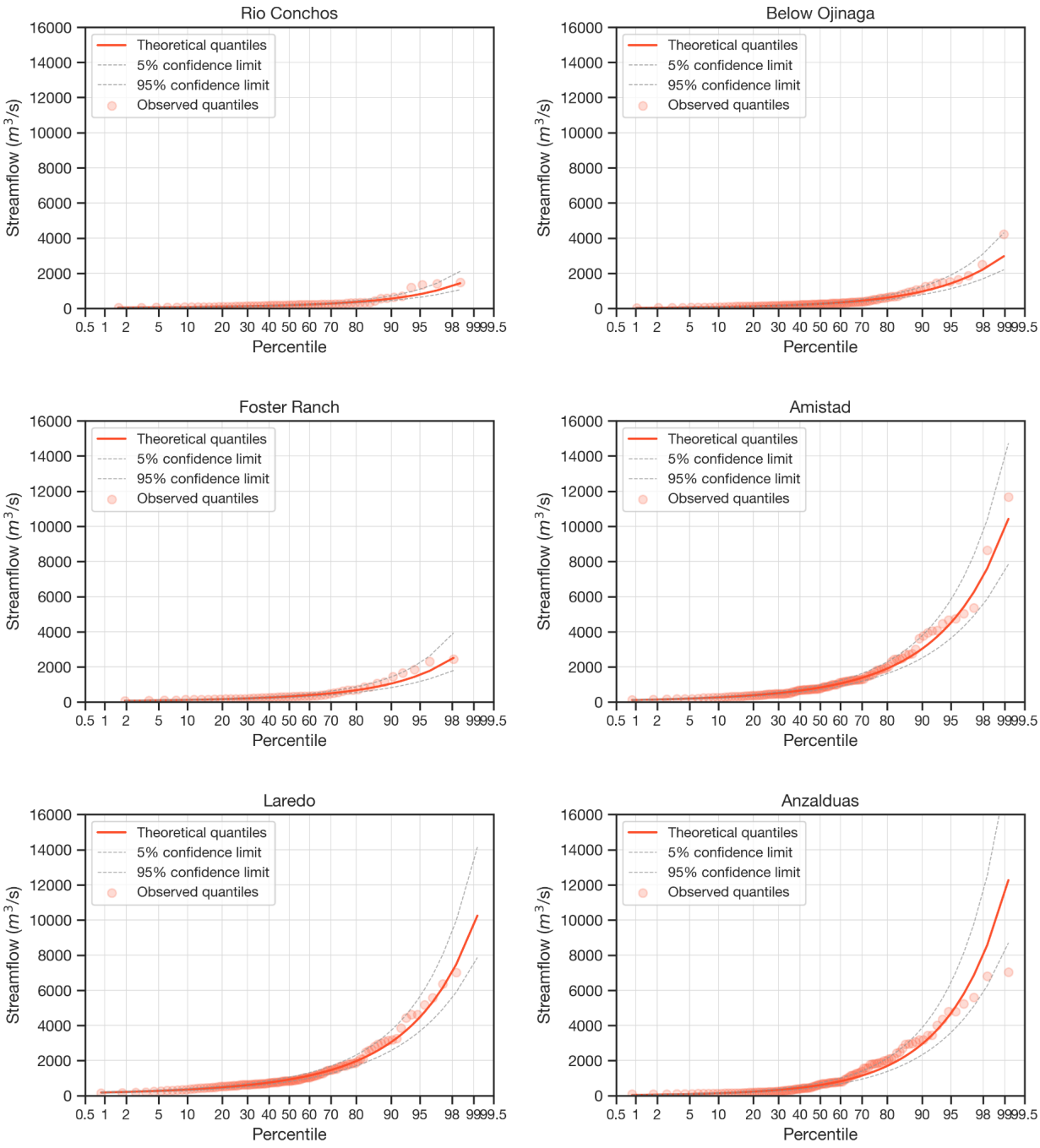


Figure 24. Probability plots with 5% and 95% confidence intervals of the regulated peak flow data series to the LP3 distribution function.

## Relationship between peak-flow magnitude and annual streamflow

To predict annual peak flows based on median annual streamflow, the median annual streamflow was estimated in moving windows of 20 years. Each median streamflow value was paired with its 20-year annual peak flow estimate for a return period of 10 years. This was plotted to observe correlation between peak flow estimate and annual streamflow, for both natural and regulated peak flows.

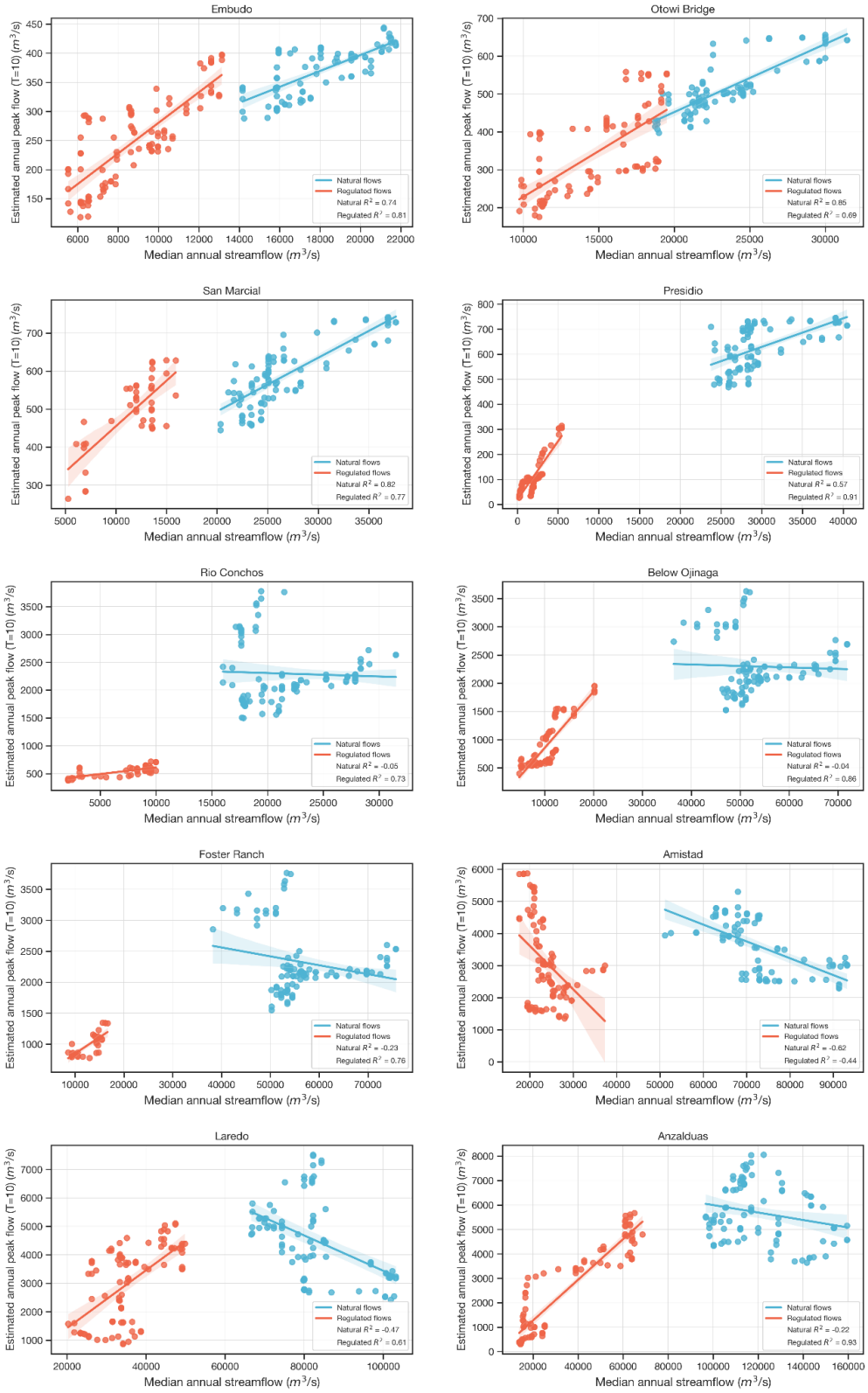


Figure 25. Correlation between the 20-year median annual streamflow and the estimated annual peak flow with a 10-year return period for natural and regulated streamflow.

# Flood event characteristics in the Northern and Southern branches of the Rio Grande-Bravo Basin

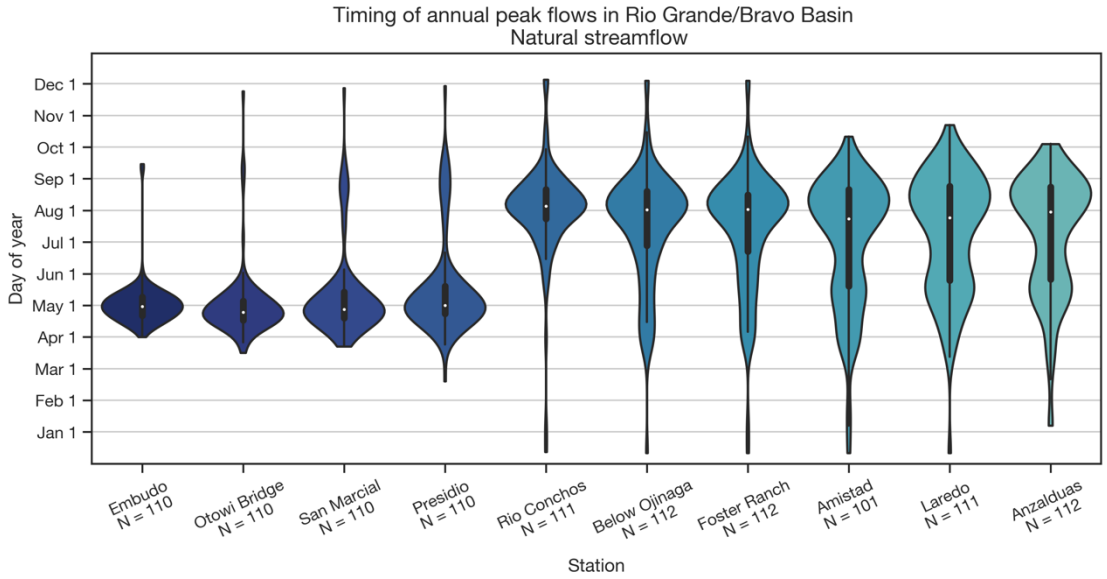


Figure 26. Timing of natural floods in the northern and southern branches of the Rio Grande-Bravo Basin.

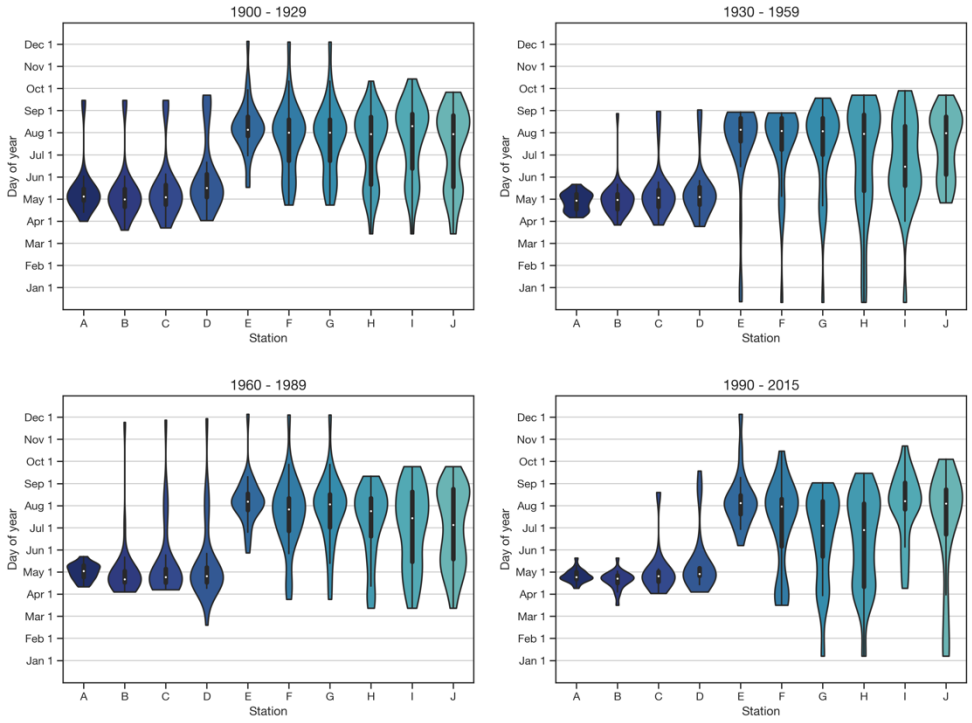


Figure 27. Timing of natural floods in the northern and southern branches of the Rio Grande-Bravo Basin in windows of 25 years.

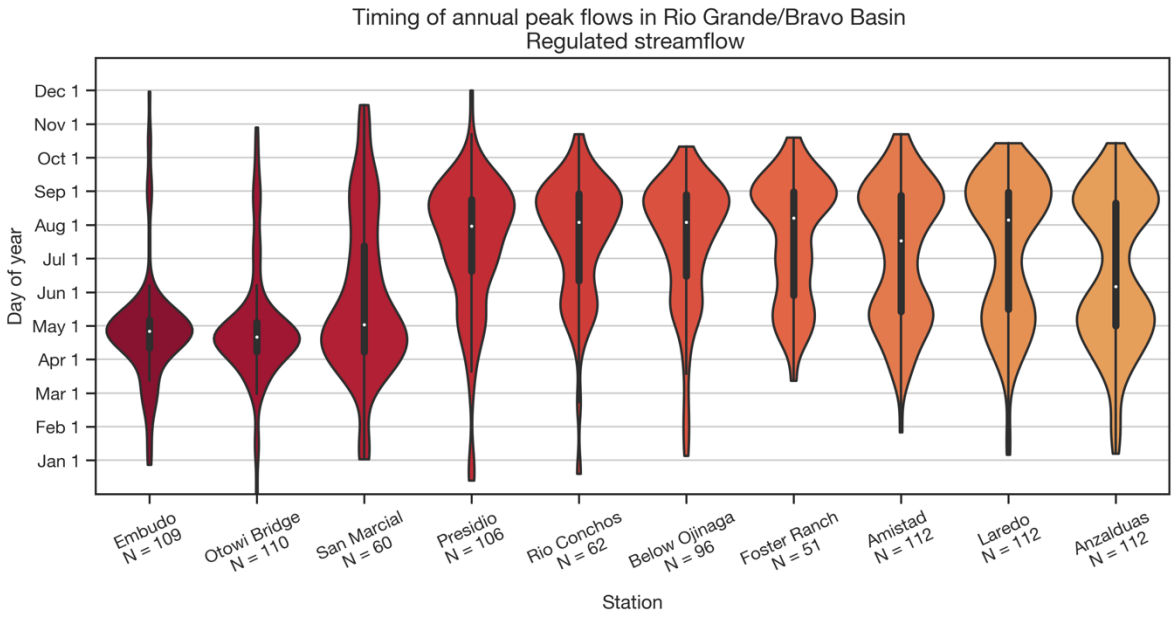


Figure 28. Timing of regulated floods in the northern and southern branches of the Rio Grande-Bravo Basin.

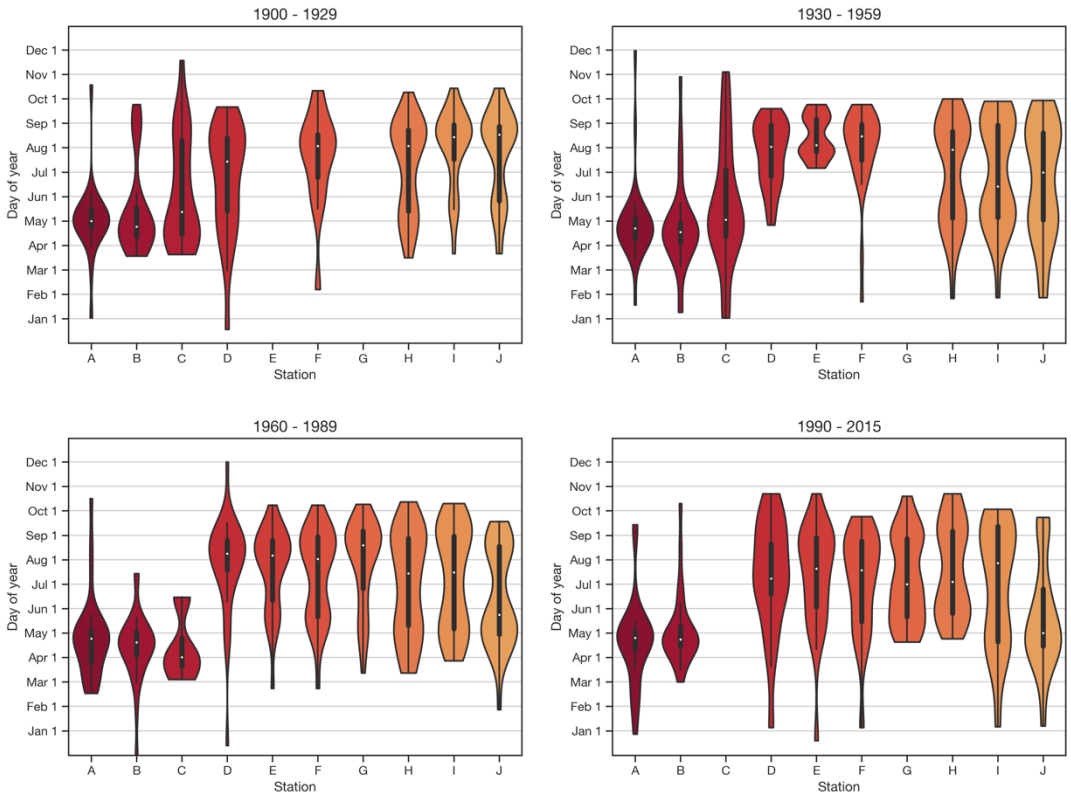


Figure 29. Timing of regulated floods in the northern and southern branches of the Rio Grande-Bravo Basin in windows of 25 years.

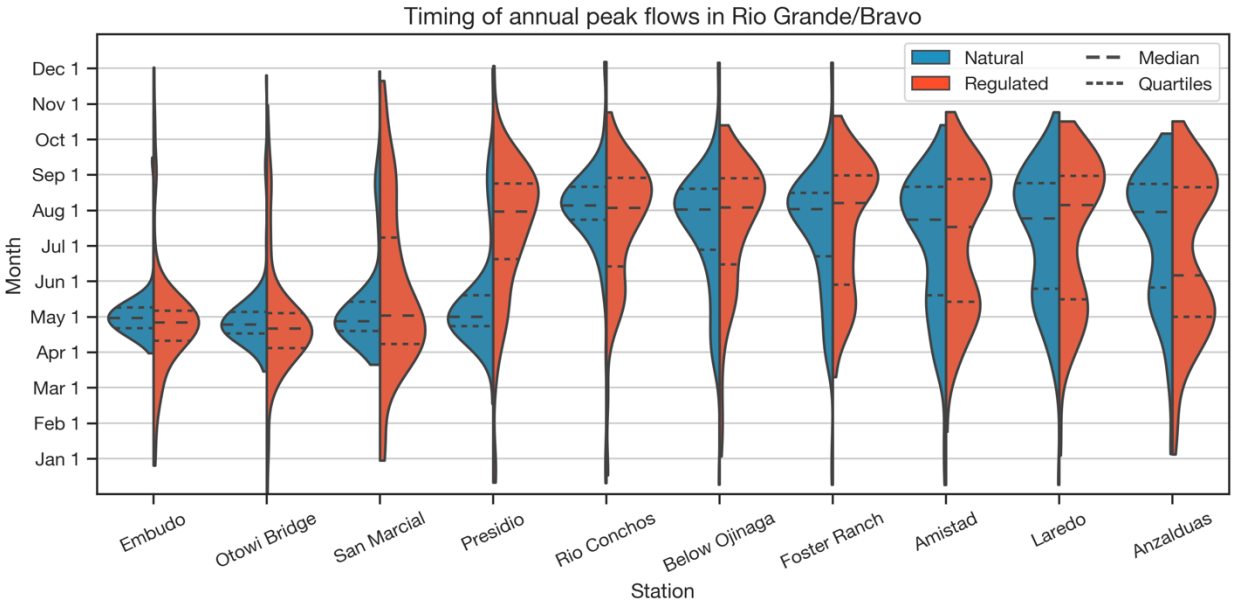


Figure 30. Timing of natural and regulated peak flows in the northern and southern branches of the Rio Grande-Bravo Basin.

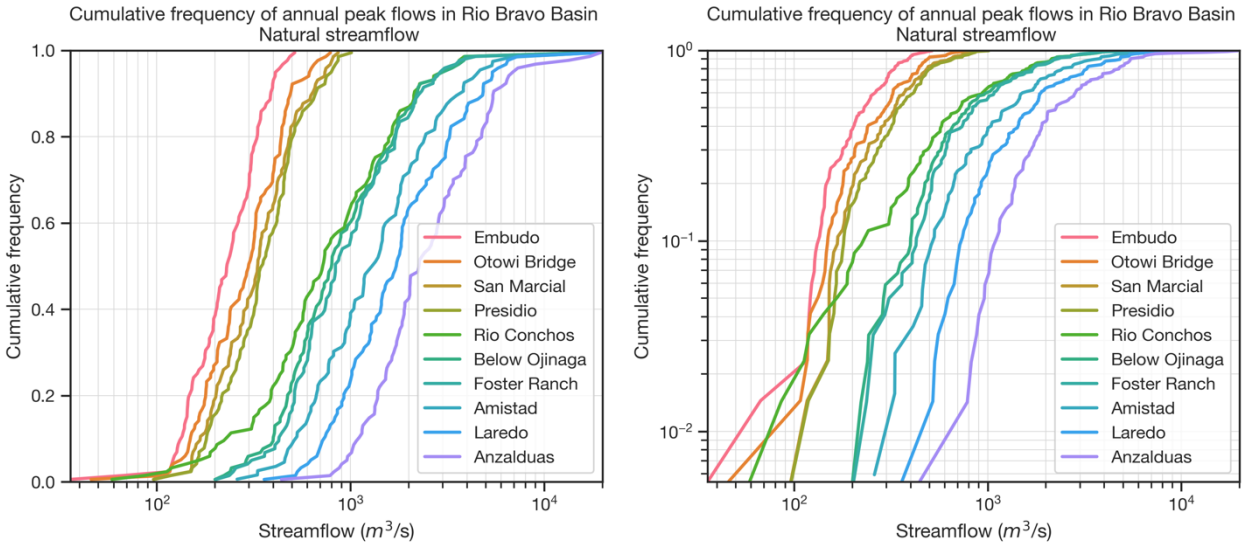


Figure 31. Exceedance probability curves of the natural flood events (northern and southern branches). Left figure: horizontal axis with logarithmic scale. Right: horizontal and vertical axis with logarithmic scale.

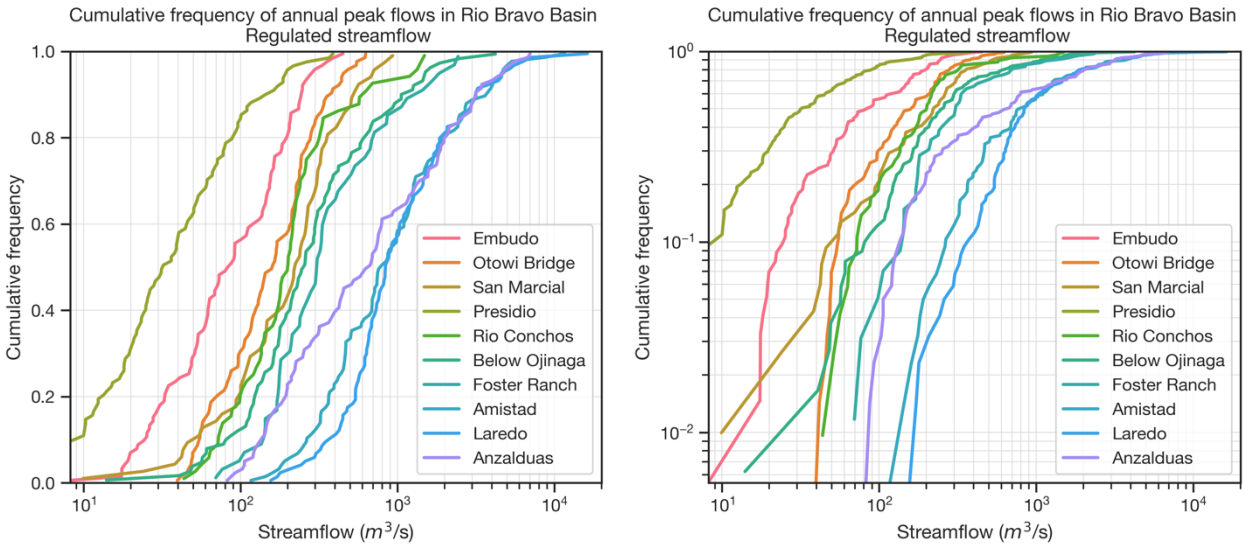


Figure 32. Exceedance probability curves of the regulated flood events (northern and southern branches). Left figure: horizontal axis with logarithmic scale. Right: horizontal and vertical axis with logarithmic scale.

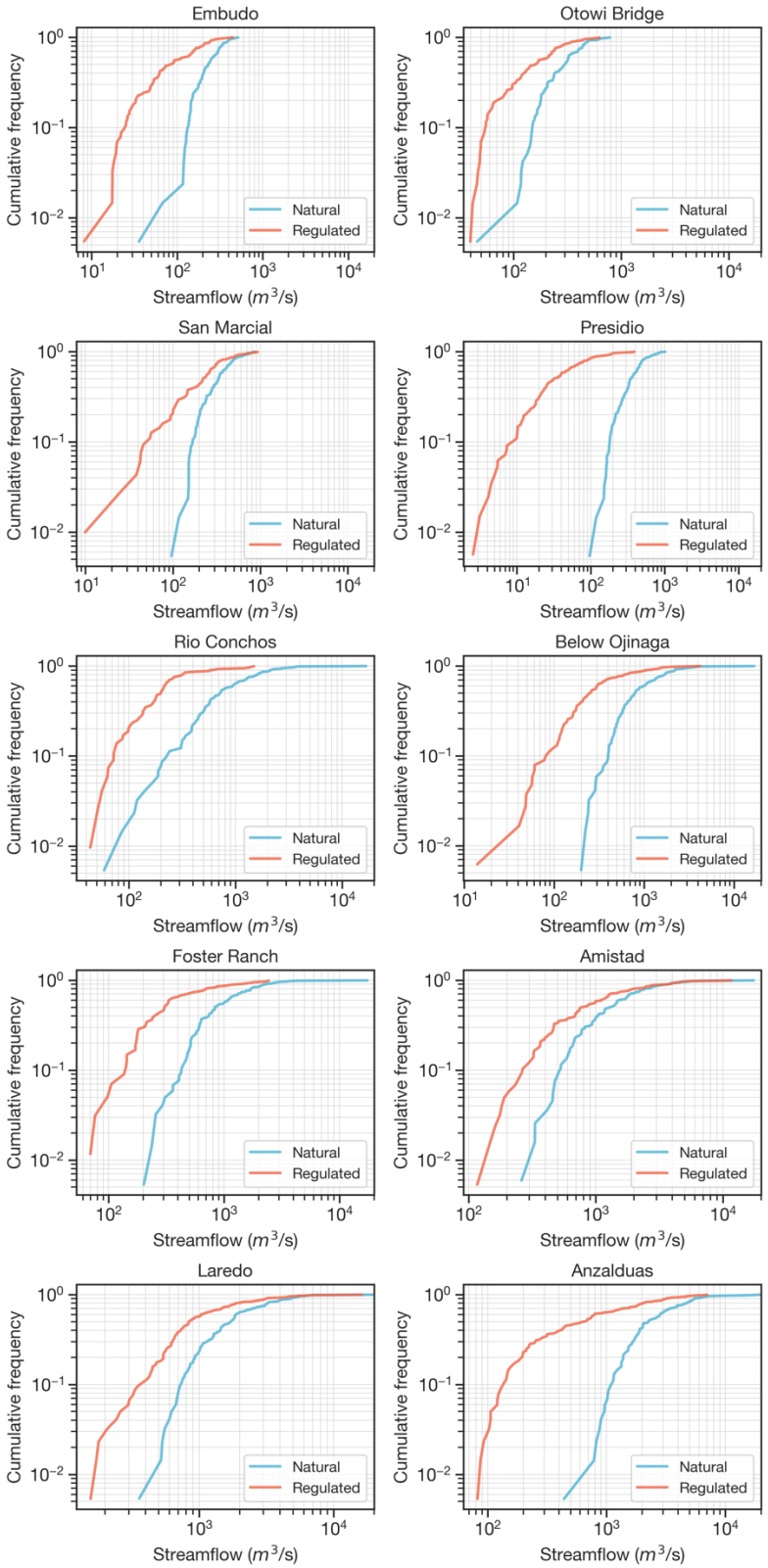


Figure 33. . Exceedance probability curves of the natural and regulated floods in the northern and southern branches, with both axis in a logarithmic scale.

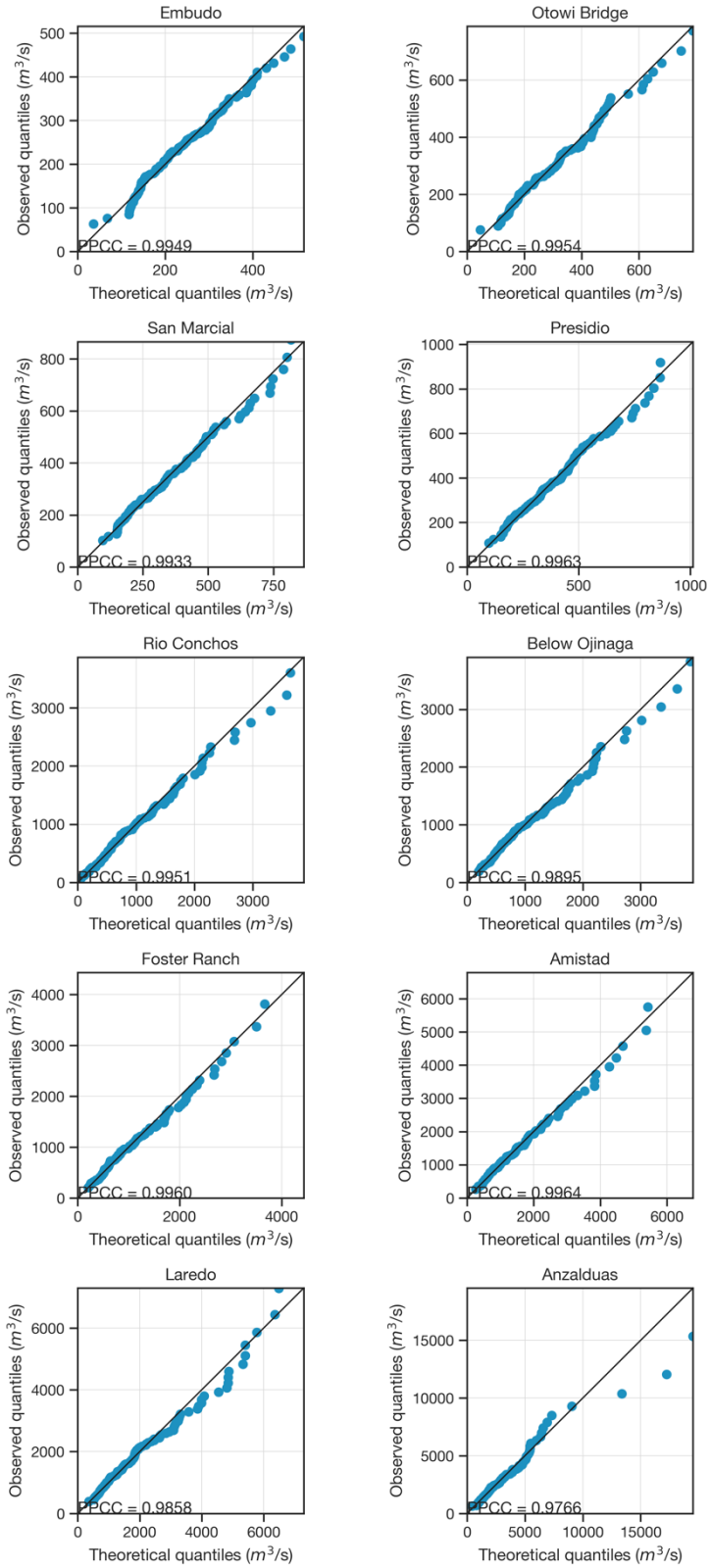


Figure 34. Quantile-quantile plots and Probability Plot Correlation Coefficient of the natural peak flow data series to the LP3 distribution function (northern and southern branches).

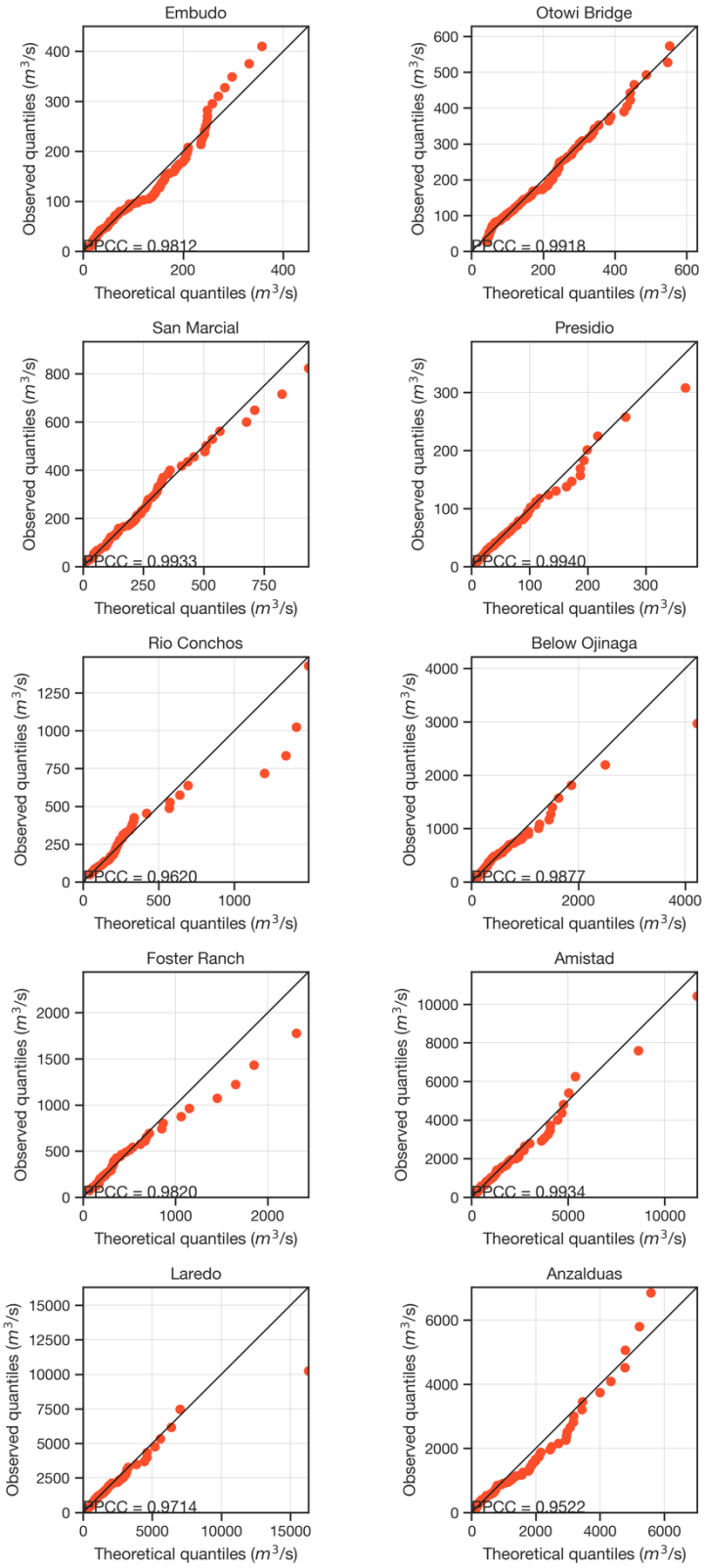


Figure 35. Quantile-quantile plots and Probability Plot Correlation Coefficient of the regulated peak flow data series to the LP3 distribution function (northern and southern branches).

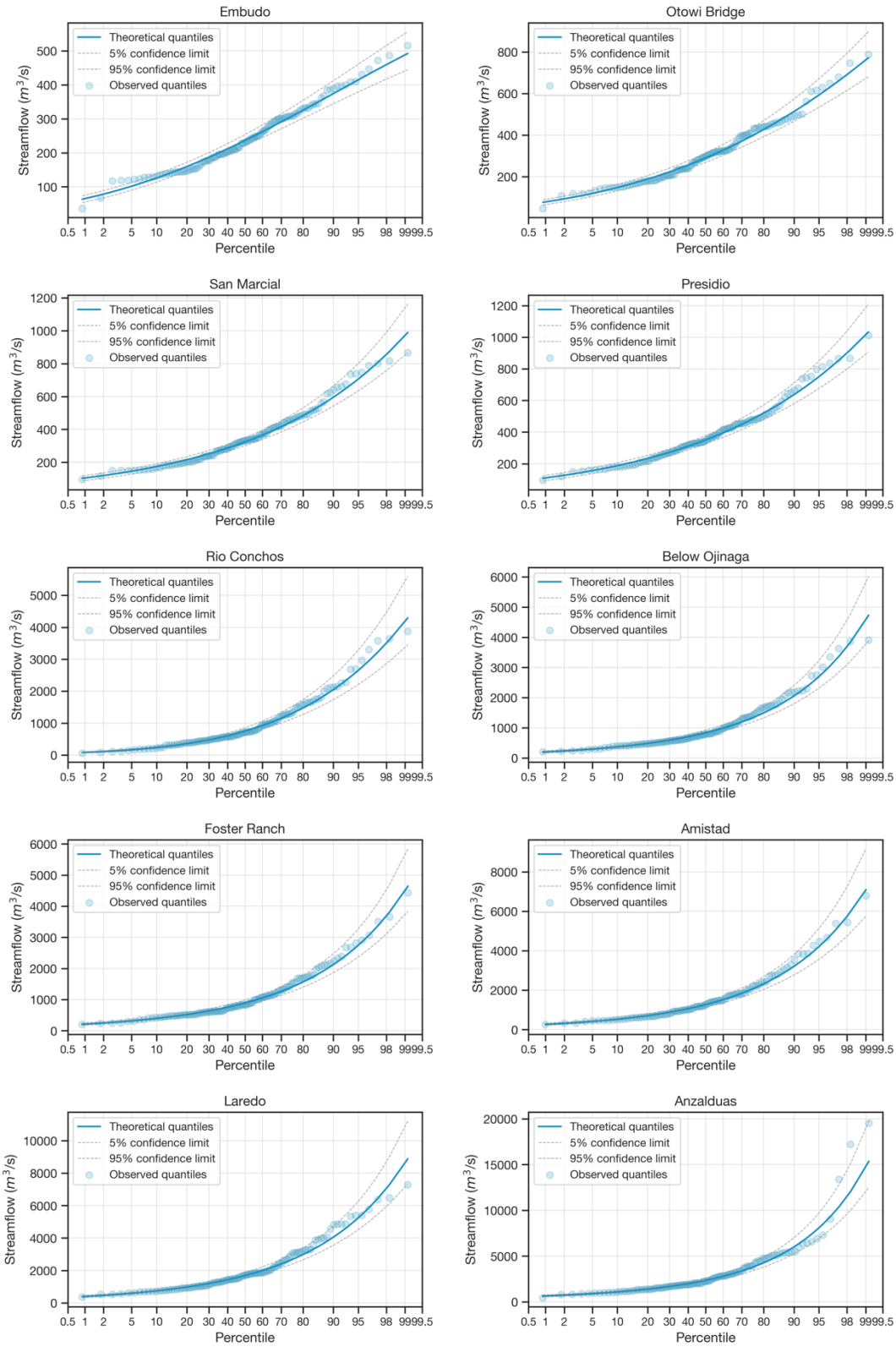


Figure 36. Probability plots with 5% and 95% confidence intervals of the natural peak flow data series to the LP3 distribution function (northern and southern branches).

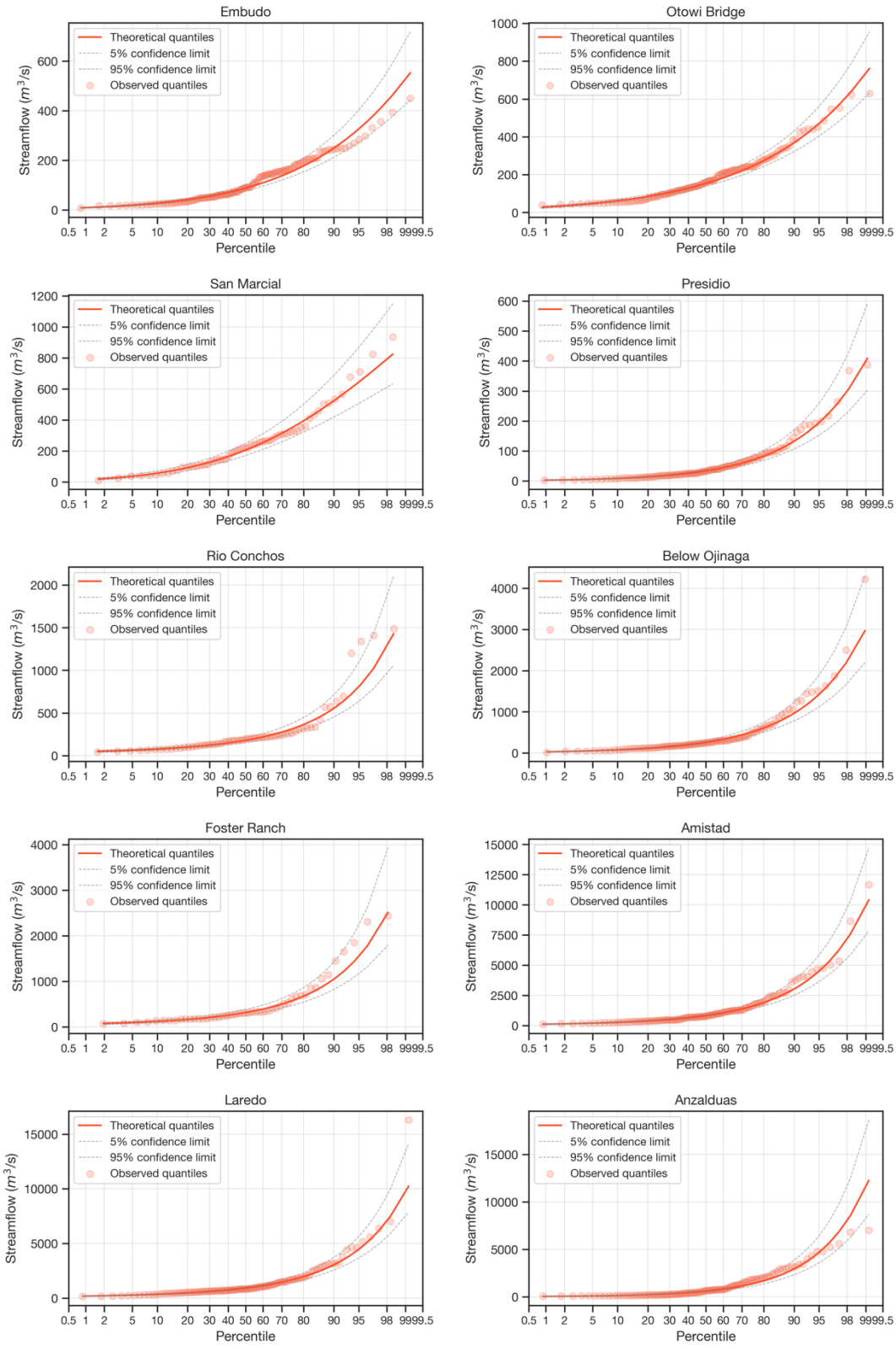


Figure 37. Probability plots with 5% and 95% confidence intervals of the regulated peak flow data series to the LP3 distribution function (northern and southern branches).

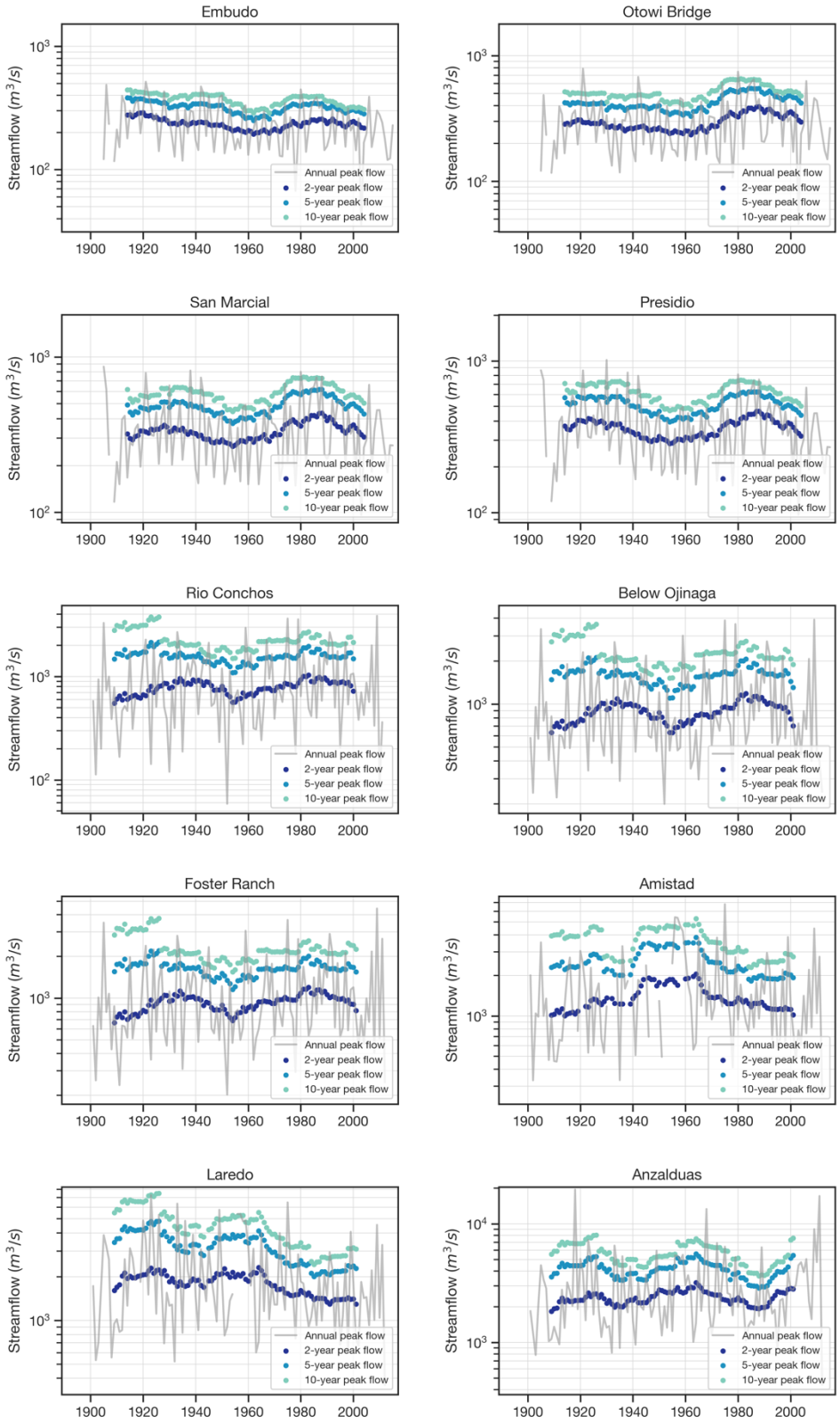


Figure 38. Estimated 2-, 5- and 10-year flood magnitude for natural streamflow for the northern and southern branches.

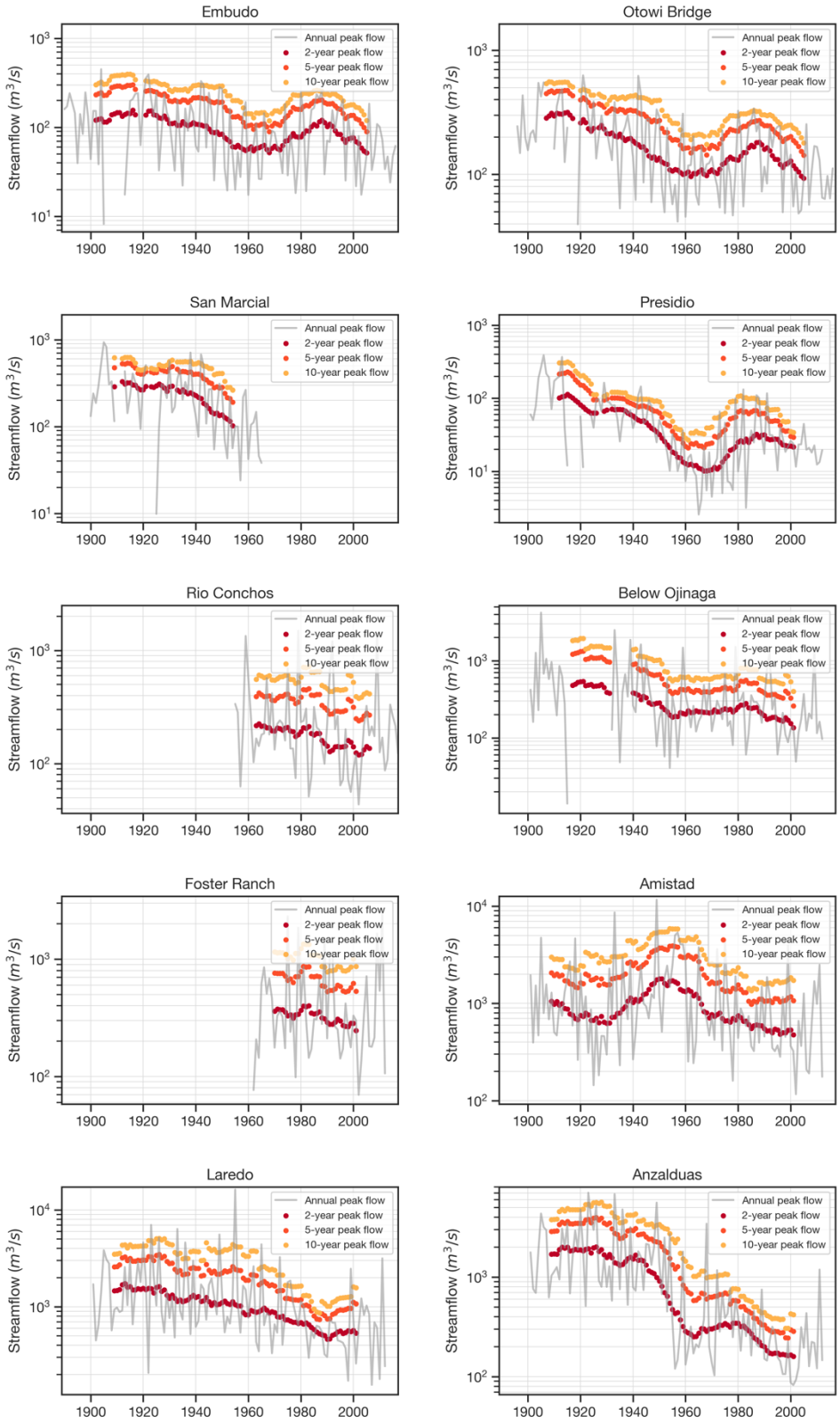


Figure 39. Estimated 2-, 5- and 10-year flood magnitude for regulated streamflow for the northern and southern branches.

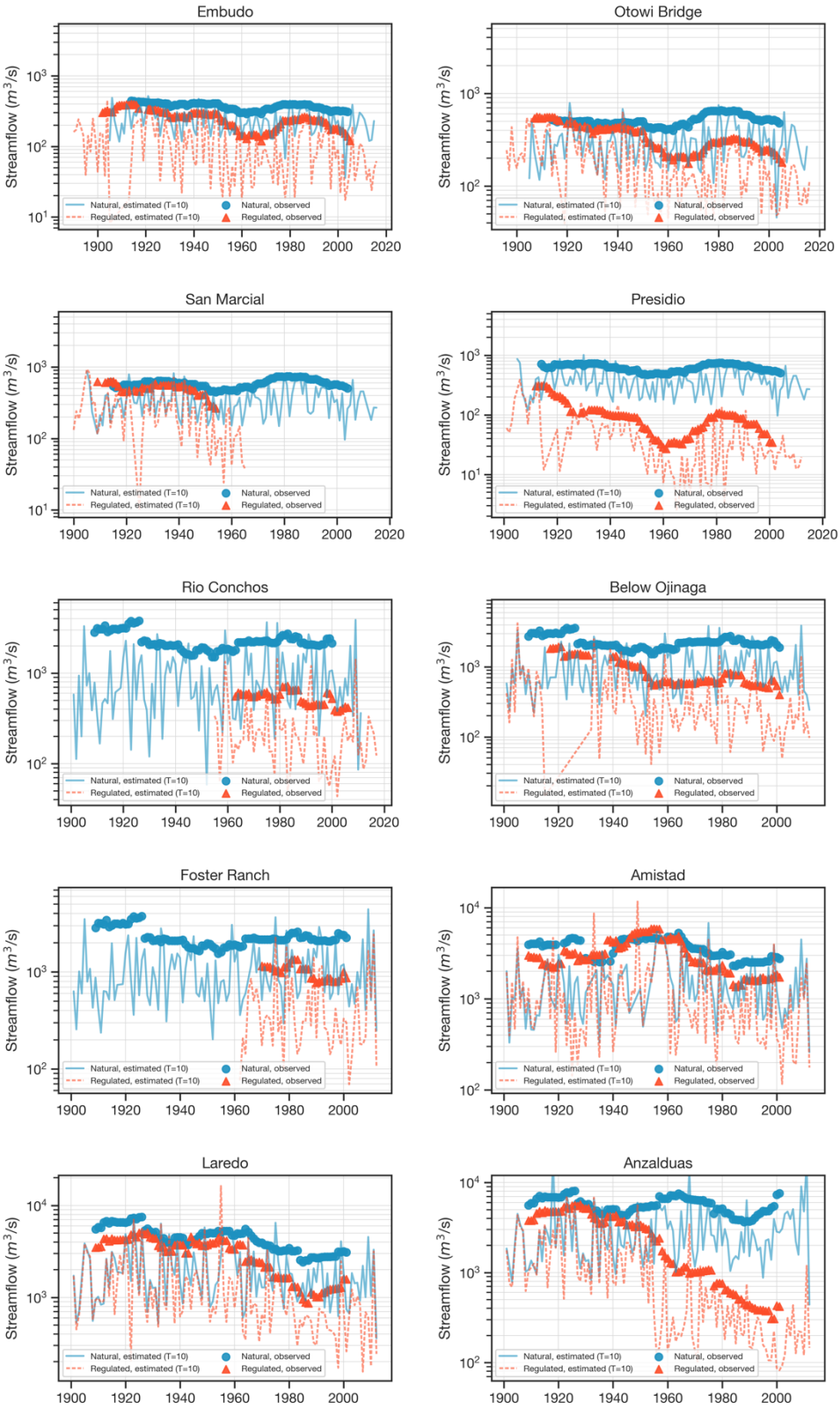


Figure 40. Estimated 10-year flood magnitude for natural and regulated streamflow for the northern and southern branches.

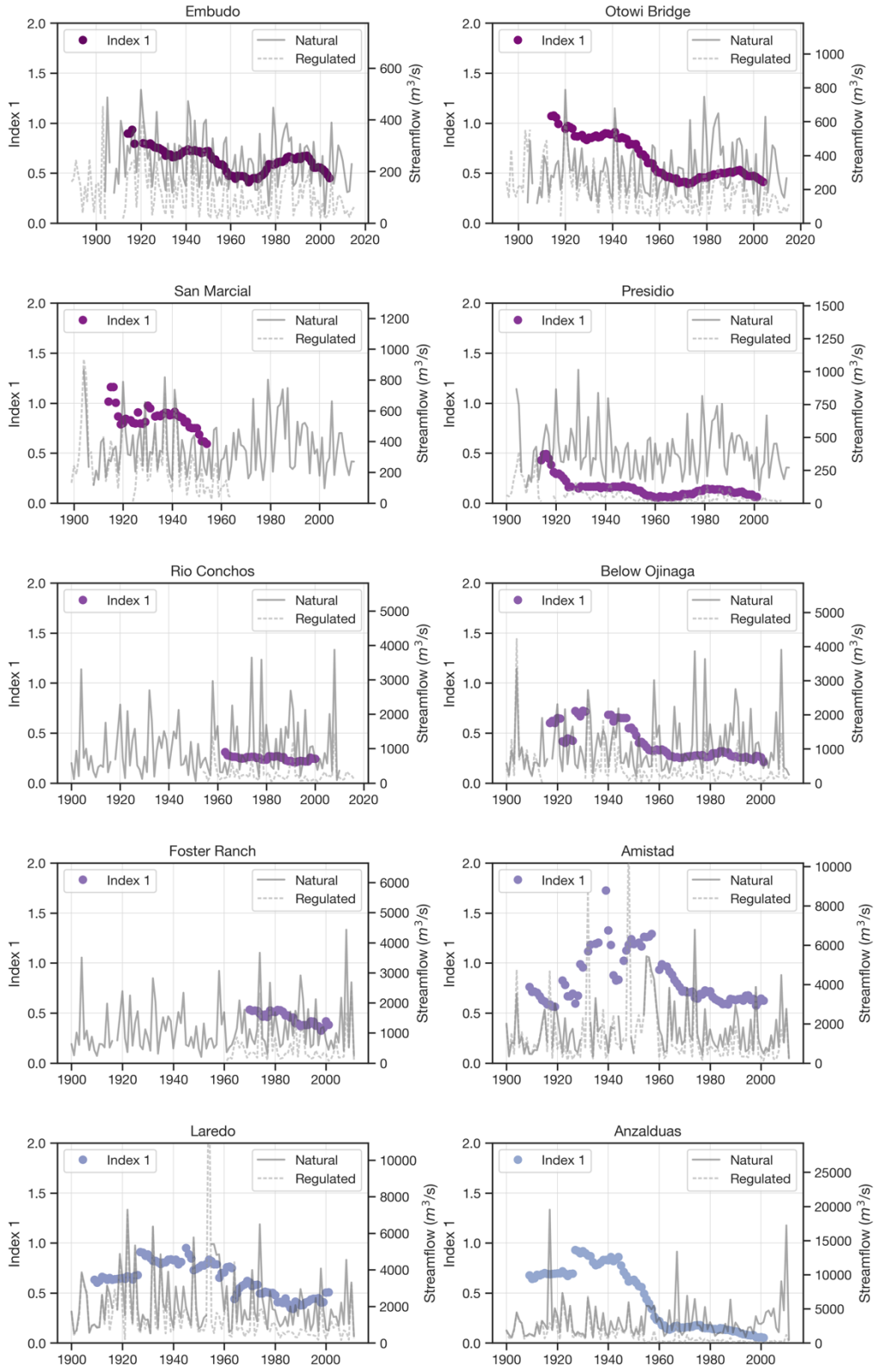


Figure 41. Index 1, comparing the changes in flood magnitude at the northern and southern branches of the Rio Grande-Bravo Basin.

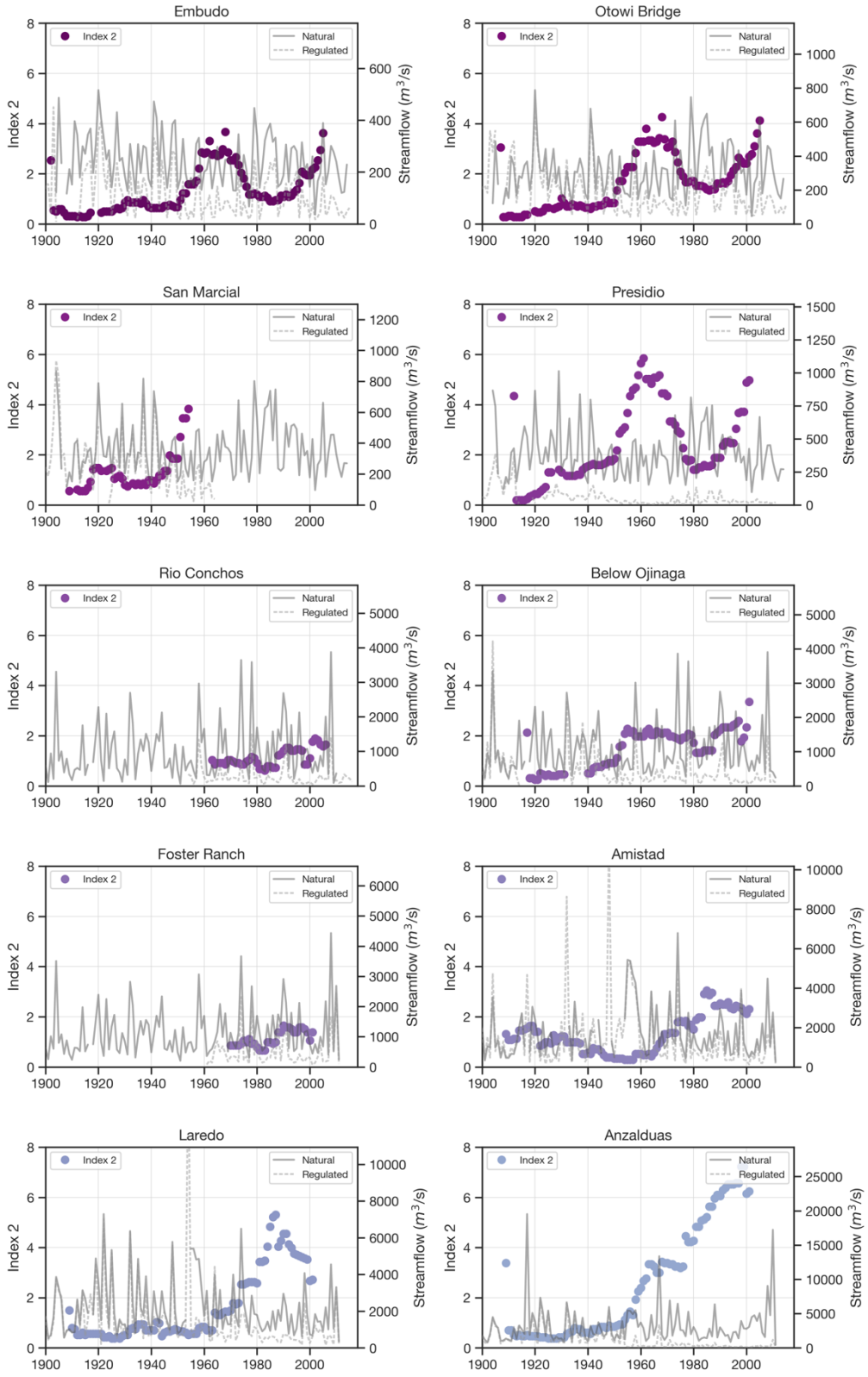


Figure 42. Index 2, comparing the changes in flood frequency at the northern and southern branches of the Rio Grande-Bravo Basin.